Microdiversity of the Vaginal Microbiome is Associated with Preterm Birth

Jingqiu Liao[1,2*†], Liat Shenhav[3*], Julia A. Urban[1], Myrna Serrano[4,5], Bin Zhu[4,5], Gregory A. Buck[4,5,6], Tal Korem[1,7,8†]

[1] Program for Mathematical Genomics, Department of Systems Biology, Columbia University Irving Medical Center, New York, NY, USA
[2] Department of Civil and Environmental Engineering, Virginia Tech, Blacksburg, VA, USA
[3] Center for Studies in Physics and Biology, Rockefeller University, New York, NY, USA
[4] Department of Microbiology and Immunology, School of Medicine, Virginia Commonwealth University, Richmond, VA, USA
[5] Center for Microbiome Engineering and Data Analysis, Virginia Commonwealth University, Richmond, VA, USA
[6] Department of Computer Science, School of Engineering, Virginia Commonwealth University, Richmond, VA, USA
[7] Department of Obstetrics and Gynecology, Columbia University Irving Medical Center, New York, NY, USA
[8] CIFAR Azrieli Global Scholars program, CIFAR, Toronto, Canada

* These authors contributed equally to this work.
[†] Corresponding authors: Emails: liaoj@vt.edu, tal.korem@columbia.edu

Abstract

Preterm birth (PTB) is the leading cause of neonatal morbidity and mortality. The vaginal microbiome has been associated with PTB, yet the mechanisms underlying this association are not fully understood. Understanding microbial genetic adaptations to selective pressures, especially those related to the host, may yield new insights into these associations. To this end, we analyzed metagenomic data from 705 vaginal samples collected longitudinally during pregnancy from 40 women who delivered preterm spontaneously and 135 term controls from the Multi-Omic Microbiome Study-Pregnancy Initiative (MOMS-PI[1]). We find that the vaginal microbiome of pregnancies that ended preterm exhibits unique genetic profiles. It is more genetically diverse at the species level, a result which we validate in an additional cohort, and harbors a higher richness and diversity of antimicrobial resistance genes, likely promoted by transduction. Interestingly, we find that *Gardnerella* species, a group of central vaginal pathobionts, are driving this higher genetic diversity, particularly during the first half of the pregnancy. We further present evidence that *Gardnerella* spp. undergoes more frequent recombination and stronger purifying selection in genes involved in lipid metabolism. Overall, our results reveal novel associations between the vaginal microbiome and PTB using population genetics analyses, and suggest that evolutionary processes acting on the vaginal microbiome may play a vital role in adverse pregnancy outcomes such as preterm birth.

Introduction

Preterm birth (PTB), childbirth at <37 weeks of gestation, is the leading cause of neonatal morbidity and mortality[2]. Each year, approximately 15 million infants are born preterm globally, over 500,000 of them

in the US[3]. Preterm infants are at a high risk of respiratory, gastrointestinal and neurodevelopmental complications[4]. While a number of maternal, fetal, and environmental factors have been associated with PTB[2,5,6], its etiopathology remains largely unknown, and early diagnosis and effective therapeutics are still lacking.

Over the past decades, growing evidence has pointed to potential involvement of the vaginal microbiome in PTB[1,7–10]. This involvement has so far been mostly characterized as an ecological process, meaning changes in microbial abundances and vaginal community states. For instance, increased richness and diversity of microbial communities and the presence of particular community state types (CST), have been repeatedly associated with PTB[1,9,11–15]. In addition, vaginal microbiomes of women who delivered preterm appear to be less stable during pregnancy, with some studies reporting a significant decrease in the richness and diversity of these microbial communities during pregnancy[1,12].

Multiple endogenous factors, such as hormonal changes, nutrient availability and microbial interactions, and exogenous factors, such as genital infections, antibiotic treatment and exposure to xenobiotics, could trigger ecological processes and alter the vaginal microbial composition[16,17]. These factors may also act as selective pressures that affect genetic variation in the microbial populations that make the vaginal microbiome. Such adaptive evolution in the vaginal environment, even during pregnancy, is highly plausible given the high mutation rates, short generation times, and large population sizes of microbes[18]. They are further supported by observations of rapid adaptation to environmental changes in other human-associated microbial ecosystems[19–21]. The way by which vaginal microbes respond to various selective pressures may, in turn, affect the host, including pregnancy outcomes. Therefore, a comprehensive investigation of the genetic diversity of the vaginal microbiome at the population level, which we term “microdiversity”, and the underlying evolutionary forces that shape it, holds promise for a better understanding of the etiopathology of PTB.

Here, we performed an in-depth population genetics analysis and characterized the population structure of the vaginal microbiome along pregnancy and in the context of preterm birth. We used metagenomic sequencing data from 705 vaginal samples collected longitudinally during pregnancy as part of the Multi-Omic Microbiome Study-Pregnancy Initiative (MOMS-PI[1]). Our analyses include samples from 40 women who subsequently experienced spontaneous preterm birth (sPTB) and 135 women who had a term birth (TB). We show that the vaginal microbiome of pregnancies that ended preterm exhibits higher nucleotide diversity at the species level and higher antimicrobial resistance potential. We find that this higher nucleotide diversity is driven by *Gardnerella* spp., a group of central vaginal pathobionts, especially during the first half of pregnancy, and suggest that this may be related to optimization of growth rates in this taxon. We further identify a strong association between evolutionary signatures and sPTB in *Gardnerella* spp., including more frequent homologous recombination and stronger purifying selection. Overall, our results show novel associations between the vaginal microbiome and sPTB at the population genetics level, and suggest that evolutionary processes acting on the vaginal microbiome may play a critical role in sPTB, and potentially also in other adverse pregnancy outcomes.

Results

The phylogenetic composition of the vaginal microbiome associates with sPTB.

We assembled a total of 1,078 metagenome-assembled genomes (MAGs) with at least medium quality[22] (>50% completeness, <10% contamination; **Supplementary Table 1**; Methods) from previously published[1] metagenomic reads generated from 705 vaginal samples[1]. These samples were collected from 175 women visiting maternity clinics in Virginia and Washington at various time points along pregnancy[1], with an average of 3.36 and 3.21 samples for women delivering preterm and at term, respectively (**Supplementary Table 2**). We clustered these MAGs into 157 species-level phylogroups at the level of 95% average nucleotide identity (ANI), which roughly corresponds to the species level[23]; and selected the most complete MAG with the least contamination as the representative for each phylogroup. These representative MAGs were 86±14% (mean±SD) complete and 1.1±1.8% contaminated, with 93 (59% of 157) of them estimated to have high quality[22] (>90% completeness and <5% contamination; **Supplementary Table 1**). Taxonomic assignment of these representative MAGs (Methods) revealed that the phylogroups represent at least 8 phyla, with genome size (adjusted by completeness) ranging from 0.6 to 7.4 Mbps and GC content ranging from 25.3% to 69.7% (**Fig. 1a**, **Supplementary Table 1**). *Actinobacteria* had the most phylogroups detected in the samples, followed by *Firmicutes* and *Bacteroidetes* (**Fig. 1a**).

Of note, 12 of these species-level phylogroups (PG042-PG053) were assigned to *Gardnerella vaginalis* according to CheckM[24], supporting the existence of multiple genotypes at the species level within the 'species' *G. vaginalis*[25,26]. To better resolve the classification of these *G. vaginalis* phylogroups, we compared the average nucleotide identity (ANI) for the representative MAGs of these phylogroups against updated reference genomes for *Gardnerella*, including *G. vaginalis*, *G. piotti*, *G. leopoldii*, *G. swidsinskii*, and nine species remained to be characterized (gs2-3 and gs7-13)[25]; gs-2-3 and gs7-13 correspond to group 2-3 and 7-13 shown in Fig. 1 in [25]. The ANI analysis shows that PG043 represents *G. vaginalis*, PG044 represents *G. swidsinskii*, PG042 represents *G. piotti*, and PG046, PG049, PG051 and PG053 represent *G.* gs7, *G.* gs8, *G.* gs13 and *G.* gs12, respectively (**Supplementary Fig. 1**). The remaining phylogroups (PG045, PG047, PG048, PG050, and PG052) do not cluster with any reference species and may represent novel species of *Gardnerella*. Here, we refer to phylogroups PG042-PG053 as *Gardnerella* spp.

To understand if the temporal dynamics of the vaginal microbiome is associated with sPTB, we employed compositional tensor factorization (CTF)[27] to assess temporal changes to the composition of the microbiome during pregnancy. This analysis shows a significant separation of women by pregnancy outcomes (PERMANOVA F = 8.0492; P = 0.002; **Fig. 1b-e**) based on the dynamics of their microbiome composition over time (**Fig. 1e)**, and specifically observed for component 1 in the CTF analysis (Mann-Whitney P = 0.015; **Fig. 1c**). We further found that the top features contributing to this difference belong to *Lactobacillus helveticus* (PG081), *Lactobacillus crispatus* (PG080), *Lactobacillus gasseri* (PG079), and *Lactobacillus jensenii* (PG076 and PG077) that are associated with TB and *Megasphaera genomosp*. (PG061), *Gardnerella* spp. (PG047, PG050, PG052), and *Atopobium vaginae* (PG041) that are associated with PTB (**Fig. 1d**); these species were previously found to be associated with pregnancy outcomes[1,9,28]. These results suggest that the vaginal microbiome has a different temporal trajectory during pregnancies ending preterm, consistent with previous findings[1,7], and with *Gardnerella* as an important factor. Overall, our results demonstrate that de-novo metagenomic analysis replicates and expands previous findings with respect to associations between the composition of the vaginal microbiome and sPTB.

Next, we sought to examine the diversity of microbial strains detected within species, and its association with sPTB. We performed the analysis on all phylogroups and found that the strains of *M. genomosp.* showed significantly higher ANI between women who delivered preterm, compared to a null distribution calculated based on ANIs from any two randomly selected women (Permutation $P = 0.002$, adjusted $P < 0.05$; Methods), a relationship not observed between women who delivered at term ($P = 0.208$; **Supplementary Fig. 2**). This result indicates that *M. genomosp.* were more closely related than expected by chance across women who delivered preterm. It suggests that sPTB-associated vaginal conditions across women may be more conserved, harboring a group of significantly closely related *M. genomosp.* strains, compared to TB-associated vaginal conditions.

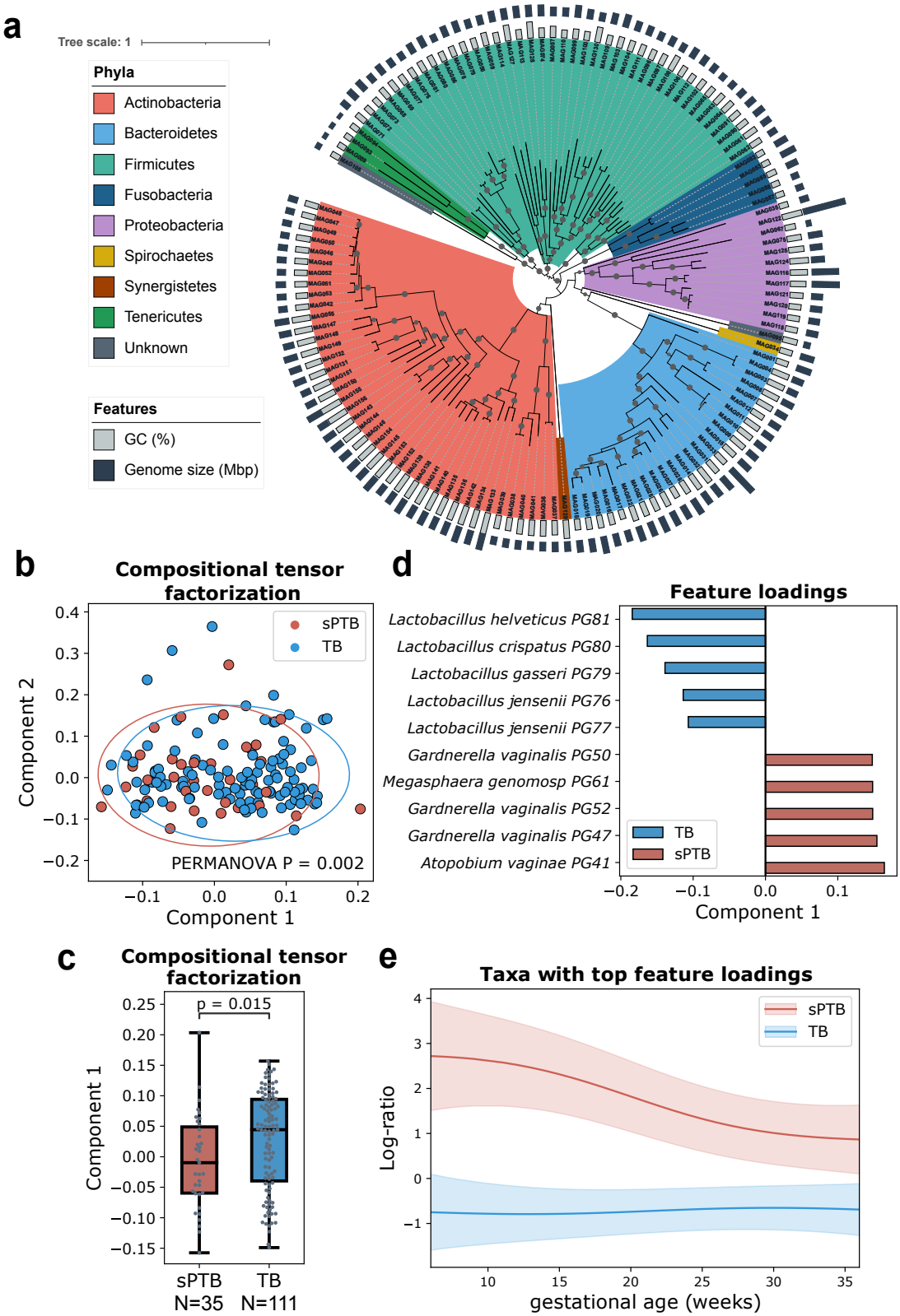

Fig. 1 | The composition of the vaginal microbiome associated with sPTB. a. Phylogenetic tree of non-redundant MAGs representing 132 species-level phylogroups differing by at least 95% average nucleotide identity (ANI) based on concatenated amino acid (AA) sequences of 120 marker genes. Representative MAGs of 25 phylogroups had <60% of marker genes AA sequence identified and were not included in the tree. Gray

154 nodes indicate a bootstrap value >80. The tree is rooted by midpoint and annotated by the GC content and
155 genome size of the representative MAGs. **b.** Compositional tensor factorization (CTF) analysis showing
156 microbiome composition trajectories over gestational ages separated by pregnancy outcomes using the top two
157 ordination axes (Component 1 and Component 2). Each dot represents a subject. **c.** Component 1 in the CTF
158 analysis compared between sPTB and TB. Box, IQR; line, median; whiskers, 1.5*IQR; *p*, two-sided Mann-
159 Whitney. **d.** Feature rankings of phylogroups colored by preterm birth (sPTB) and term birth (TB) based on
160 Component 1 in the CTF analysis. **e.** Log ratio of top and bottom taxa from (d) over time, separated to PTB and
161 TB samples. Shaded area, 95% CI.
162
163
164 **The microdiversity of the vaginal microbiome is higher in the first half of pregnancies that**
165 **ended preterm, driven by *Gardnerella* species.**
166
167 Human microbes can adapt to host-induced environmental changes (e.g., diet, antibiotics) through
168 genetic variations[29]. Therefore, the microbial populations of the same species in different hosts can
169 have a different genetic structure, which provides them a competitive advantage. These genetic
170 differences, in turn, may be related to the phenotype of the host. To understand the genetic structure of
171 microbial populations in the vaginal environment and its association with pregnancy outcomes, we
172 calculated the nucleotide diversity for each identified phylogroup. Overall, vaginal microbial populations
173 had a significantly higher genome-wide nucleotide diversity in sPTB than in TB (median along
174 pregnancy; Mann-Whitney $P = 0.0073$; **Fig. 2a**). Stratifying by phylogroups, we found that this
175 difference was mainly driven by *Gardnerella* spp. ($P = 0.017$; **Fig. 2b**). *G. piotti* (PG042), *G. swidsinskii*
176 (PG044), and *G*. gs13 (PG051) and a potentially novel *Gardnerella* spp. (PG045), along with a
177 phylogroup of *Atopobium vaginae*, a suspected vaginal pathobiont[30], showed significantly higher
178 genome-wide nucleotide diversity in sPTB ($P < 0.05$, adjusted $P < 0.1$ for all; **Supplementary Fig. 3a**).
179 These results imply that microbial populations composed of more diverse strains from the same
180 species, and particularly *Gardnerella* spp., are growing in the vaginal environment associated with
181 sPTB.
182
183 To understand how the nucleotide diversity of *Gardnerella* spp. changes over time during pregnancy,
184 we analyzed temporal trajectories of term and preterm pregnancies. To this end, we pooled the data
185 from all women in each group, binned pregnancy weeks and used splines to smooth the temporal
186 curves (Methods). We found a significant difference between the temporal trajectories of *Gardnerella*
187 spp. nucleotide diversity in pregnancies ending at term and preterm (Permutation test < 0.001 (ref. [31]),
188 Wilcoxon signed-rank $P < 0.003$; Methods; Fig. 2c). Specifically, we found that the nucleotide diversity
189 of *Gardnerella* spp. increased at the beginning of pregnancies which ended preterm, with a peak at
190 around gestational week 13, and then dropped to its initial value at around gestational week 20 (**Fig.**
191 **2c**). In comparison, nucleotide diversity of *Gardnerella* spp. in TB remained relatively stable (**Fig. 2c**).
192 Given that gestational week 20 is the middle of a full-term pregnancy, we subsequently analyzed
193 samples with respect to two time periods - first half (0-19 gestational week) and second half of
194 pregnancy (20-37 gestational week; 37 was chosen to ensure a similar time range for both sPTB and
195 TB). As expected, the nucleotide diversity of *Gardnerella* spp.in sPTB was also significantly higher in
196 sPTB in the first half of pregnancy (median along first half; Mann-Whitney U $P = 0.0091$; **Fig. 2d**), but
197 not in the second half ($P = 0.71$; **Fig. 2e**). We further found that nucleotide diversity had a significantly
198 stronger correlation with synonymous mutations than with nonsynonymous mutations across
199 *Gardnerella* spp. (paired t-test $P = 0.0011$; **Supplementary Fig. 3b**), suggesting a more important role

of purifying selection in shaping genomic diversity. Overall, these results suggest that genetic diversity of *Gardnerella* spp. in the first half of pregnancy is important to birth outcomes, and could perhaps be used as a biomarker for early diagnosis of sPTB.

Analyzing microdiversity across all phylogroups in the two halves of pregnancy, we again found that it was significantly higher in sPTB in the first half of pregnancy (median along first half; Mann-Whitney U $P = 0.0036$; **Fig. 2f**), but not in the second half ($P = 0.16$; **Fig. 2g**). Notebly, we were able to replicate this analysis using data from an additional dataset of vaginal metagenomic sequencing from ten pregnant individuals[32] (median along first and second half; one-sided Mann-Whitney U $P = 0.021$ and $P = 0.12$, respectively; **Fig. 2h** and **2i**). Finally, clinical interventions for risk of preterm birth (eg., receiving cerclage or progesterone) may alter the microbiome composition, and thus confound our findings. To examine this potential bias, we repeated our analysis on 161 woman who received neither progesterone nor cerclage. Once more, we found that it was significantly higher in sPTB in the first half of pregnancy (U $P = 0.028$; **Supplementary Fig. 4a**), but not in the second half ($P = 0.12$; **Supplementary Fig. 4b**). Overall, our results demonstrate an increased nucleotide diversity in the vaginal microbiome during pregnancies that ended preterm, in a way that replicates across studies and is not biased by common clinical interventions for prevention of preterm birth.

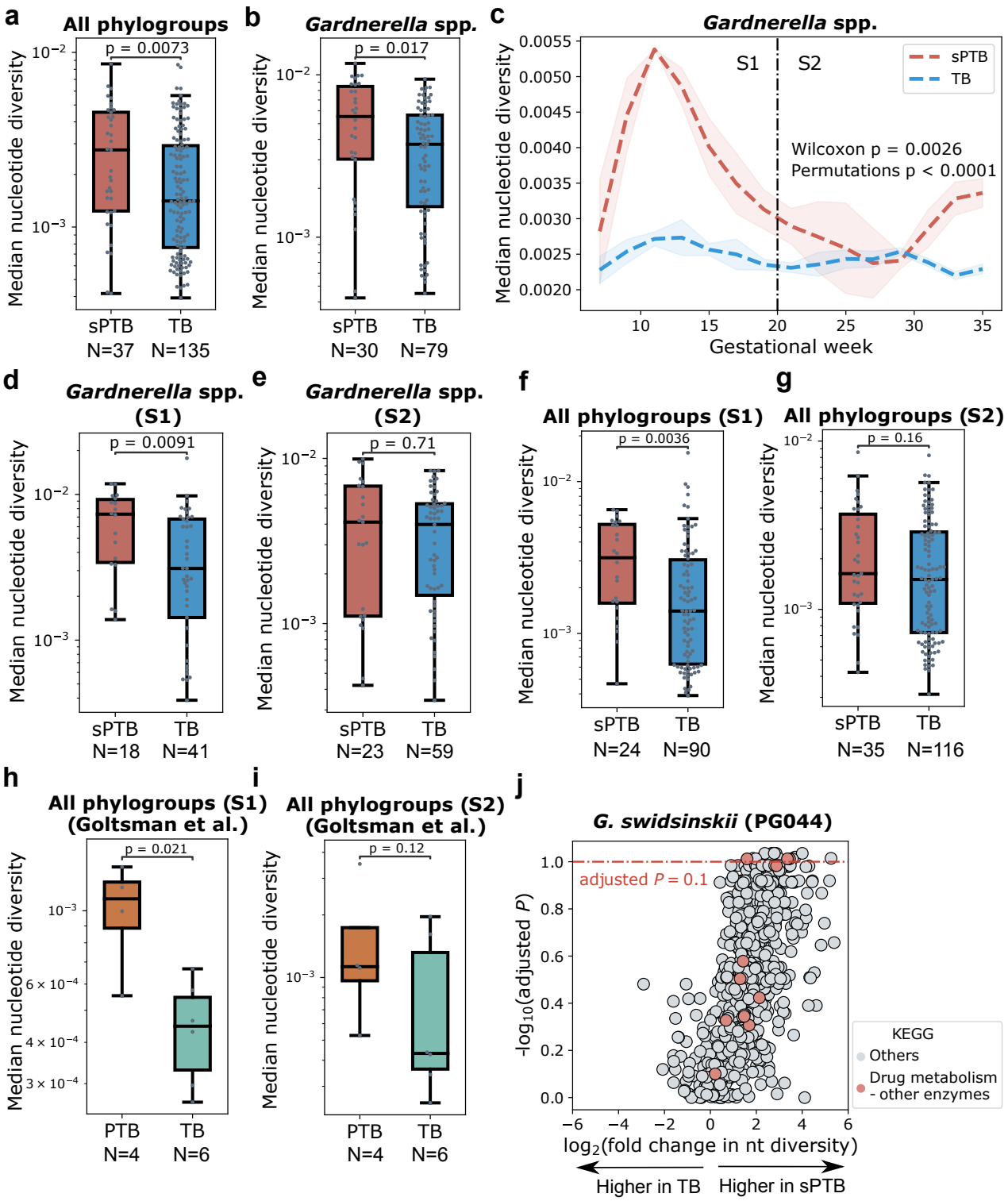

Fig. 2 | Microdiversity patterns of the vaginal microbiome are associated with sPTB. a-b, A comparison of median genome-wide nucleotide diversity along pregnancy between sPTB and TB, displayed for all phylogroups (a) and *Gardnerella* spp. (b). *p*, two-sided Mann-Whitney. **c,** Trajectory of median nucleotide diversity of *Gardnerella* spp. along pregnancy. S1 - first half of pregnancy; S2 - second half of pregnancy. The shaded area depicts mean ± s.d./n. **d-e,** A comparison of median genome-wide nucleotide diversity of *Gardnerella* spp. between sPTB and TB, displayed for pregnancy S1 (d) and S2 (e). *p*, two-sided Mann-Whitney. **f-g,** A comparison of median genome-wide nucleotide diversity of all phylogroups between sPTB and TB, displayed for pregnancy

226 S1 (f) and S2 (g). *p*, two-sided Mann-Whitney. **h-i,** Same as d-e, using data from the independent cohort of
227 Goltsman et al[32]. *p*, one-sided Mann-Whitney. Box, IQR; line, median; whiskers, 1.5*IQR. **j.** Volcano plot
228 illustrating the significance (Mann-Whitney; y-axis) of difference between nucleotide diversity (fold change; x-
229 axis) in sPTB and TB of every gene in *G. swidsinskii* (PG044). Genes above the red dashed line have $P < 0.05$ and
230 an adjusted $P < 0.1$. Genes belonging to KEGG pathways that were significantly enriched in genes showing
231 significant nucleotide diversity differences are color-coded (adjusted $P < 0.1$).
232
233 To understand if any particular genes are driving the association between sPTB and the microdiversity
234 of *Gardnerella* spp. in the first half of pregnancy, we further analyzed nucleotide diversity at the gene
235 level for these species. We identified 21 and 47 genes (out of 825 and 531) in *G. swidsinskii* (PG044)
236 and *G. vaginalis* (PG043), respectively, that showed significantly different nucleotide diversity between
237 sPTB and TB (median along the first half of pregnancy; Mann-Whitney $P < 0.05$, adjusted $P < 0.1$ for
238 all). These genes included one gene encoding the putative tail-component of bacteriophage HK97-gp10
239 ($P = 0.0012$) and one gene encoding putative AbiEii toxin, Type IV toxin–antitoxin system ($P = 5x10^{-4}$),
240 which might be involved in the interaction with maternal health[33,34]. To further identify what functions
241 were related to these associations, we then performed functional enrichment analysis (Methods) using
242 the eggNOG functional annotation of genes (**Supplementary Table 3**). We found that the KEGG
243 pathway 'drug metabolism - other enzymes' (ko00983) was significantly enriched among genes from *G.*
244 *swidsinskii* (PG044) that had significantly higher microdiversity ($P < 0.05$, adjusted $P < 0.1$; **Fig. 2j**).
245 This result suggests that the more diverse gene pool in *G. swidsinskii* (PG044) detected in sPTB may
246 be associated with adaptation to drugs present in the environment. This may be consistent with our
247 recent finding that xenobiotics detected in the vaginal environment are strongly associated with sPTB[35].
248
249 To verify that the higher nucleotide diversity we observed in sPTB pregnancies was not caused by
250 sampling or sequencing bias, we compared the read count and quality of MAGs obtained from sPTB
251 and TB samples. If this higher diversity is the result of a higher read count in sPTB samples or more
252 complete MAGs, we would expect read count and MAG completeness to be higher in sPTB samples.
253 Instead, we found the completeness and contamination of MAGs assembled from sPTB samples were
254 not significantly different from TB (Mann-Whitney $P = 0.71$ and 0.73, respectively; **Supplementary Fig.**
255 **5a,b**). Next, we assessed the correlation between the number of reads mapped to each phylogroup and
256 its genome-wide diversity. If a higher diversity is caused by more reads mapped to the MAG
257 representing the phylogroup, we would expect a positive correlation between these two measurements.
258 However, only 3 phylogroups (PG064, a *Dialister* spp.; PG102, a *Peptoniphilus* spp.; and PG122, a
259 *Bradyrhizobium* spp.) had a significant positive correlation between read counts and nucleotide
260 diversity (Spearman $\rho = 0.70$, 0.54, and 0.42, respectively; non-adjusted $P = 0.035$, 0.024, and
261 0.00015, respectively). In 98% of phylogroups, we did not observe a statistically significant positive
262 correlation (median [IQR] Spearman correlation of -0.067 [-0.19, -0.13]). None of the four *Gardnerella*
263 spp. Phylogroups that showed significantly higher nucleotide diversity in sPTB pregnancies in
264 **Supplementary Fig. 3** were significantly positively correlated (Spearman $\rho = -0.00$, -0.12, -0.02, and -
265 0.35 and P = 0.96, 0.091, 0.77, and 0.00045 for PG042, PG044, PG045, and PG051, respectively;
266 **Supplementary Fig. 5c**).
267
268 Finally, as we have observed a significantly higher read count in sPTB samples (Mann-Whitney $P =$
269 0.0004 and 0.061 for samples and subjects, respectively; **Supplementary Fig. 5d and 5e**,
270 respectively), we subsampled an identical number of reads (10^5) from each sample, retaining 75% of
271 samples, and repeated our analyses of nucleotide diversity. As with the first analysis (**Fig. 2**),

nucleotide diversity was significantly higher in sPTB pregnancies across all phylogroups, and particularly in *Gardnerella* spp.(Mann-Whitney $P = 0.015$ and $P = 0.0043$, respectively; **Supplementary Fig. 5f and 5g**, respectively). Similarly, in the first half of pregnancy, the nucleotide diversity of *Gardnerella* spp.was significantly higher in sPTB ($P = 0.026$; **Supplementary Fig. 5h**), while in the second half, there was no significant difference ($P = 0.22$; **Supplementary Fig. 5i**). We further subsampled an identical number of reads (5,000) mapped to *Gardnerella* spp. from each sample and repeated the analysis in **Fig. 2b**. A significant higher nucleotide diversity in sPTB pregnancies in *Gardnerella* spp. is still detected ($P = 0.028$; **Supplementary Fig. 5j**), indicating this association is not biased by higher coverage of reads mapped to *Gardnerella* spp. Overall, these results confirm that the sPTB-associated nucleotide diversity we observed was not biased by technical artifacts.

Evolutionary forces acting on *Gardnerella* species are associated with pregnancy outcomes.

Adaptation should increase the fitness of an organism, its ability to survive and reproduce in a given environment. To better understand if the *Gardnerella* spp. populations with higher genetic diversity grow better in the vaginal environment associated with sPTB, we inferred fitness using two measures: relative abundance and growth rate. Indeed, we found that nucleotide diversity in these species was positively correlated with relative abundance (Spearman $\rho = 0.35$, $P = 0.0013$; **Fig. 3a**). This correlation was not observed in other phylogroups (**Supplementary Fig. 6a**). *L. crispatus* (PG080) and *L. iners* (PG086) even showed a significantly negative correlation ($\rho = -0.39$ and -0.32, $P = 0.026$ and 0.0014, respectively; **Supplementary Fig. 6b,c**). We additionally used gRodon[36] to predict the maximal growth rate of microbes based on codon usage bias in highly expressed genes encoding ribosomal proteins. We found that in the first half of pregnancy, *Gardnerella* spp. had a somewhat higher, albeit not statistically significant, maximal growth rate in sPTB pregnancies (Mann-Whitney $P = 0.057$; **Fig. 3b**), while in the second half of pregnancy, the difference was diminished ($P = 0.15$; **Fig. 3c**). No significant difference in the maximal growth rate was observed in non-*Gardnerella* phylogroups ($P > 0.05$ for all). While the *in situ* growth rates[37,38] of *Gardnerella* were higher in the sPTB group during the first half of pregnancy, this difference was not statistically significant ($P = 0.08$; data not shown). These results suggest that the sPTB-associated genetic diversity observed in *Gardnerella* spp. may be related to the optimization for faster growth in the sPTB-associated vaginal environment.

Microbial population structure is influenced by various evolutionary processes including selection and homologous recombination[39]. Competence, a mechanism of horizontal gene transfer which involves homologous recombination, has been identified in *Gardnerella* spp[40]. To better interpret the significant differences we observed in the microdiversity patterns of *Gardnerella* spp. between sPTB and TB, we quantified the degree of homologous recombination using the normalized coefficient of linkage disequilibrium between alleles at two loci, D'. A value of D' closer to 0 indicates a higher degree of recombination[41]. Interestingly, we found that the median D' of *Gardnerella* spp. was significantly smaller in sPTB pregnancies in both the first (Mann-Whitney $P = 0.041$; **Fig. 3d**) and second halves of pregnancy ($P = 0.013$; **Fig. 3e**), and the same was also observed for the D' of three specific *Gardnerella* spp., *G. piotti* (PG042), *G.* gs7 (PG046), and PG047, in the first half of pregnancy ($P < 0.05$, adjusted $P < 0.1$ for all; **Supplementary Fig. 7a**). No significant difference in recombination was observed in non-*Gardnerella* phylogroups (adjusted $P > 0.1$ for all). These results suggest that *Gardnerella* spp. tends to have more frequent recombination in women who delivered preterm during both halves of pregnancy.

Next, we quantified the degree of selection using dN/dS in this species (Methods). This measure quantifies the ratio between synonymous and non-synonymous mutations, and hence offers insight into the type of selection, with values close to zero indicating purifying selection, and values higher than one indicating positive selection[42]. dN/dS is calculated in relation to the reference, and can therefore detect selection on mutations that have already been fixed within the population[43]. Consistent with the gut and ocean microbiomes[44–46], purifying selection is predominant across all genes of the vaginal microbiome (dN/dS << 1; median [IQR] dN/dS of 0.17 [0.10, 0.29]; **Supplementary Fig. 7b**). While the median dN/dS of all *Gardnerella* spp. genes was not significantly different between sPTB and TB pregnancies (Mann-Whitney U $P = 0.48$), we detected some differences when examining high-level functions (COG categories[47]) within each half of pregnancy. In the first half, the median dN/dS of *Gardnerella* spp. genes was somewhat lower in sPTB pregnancies for inorganic ion transport and metabolism, lipid transport and metabolism, secondary structure, and cell wall/membrane/envelope biogenesis, though this was not statistically significant after adjusting for multiple testing (COG categories “P”, “I”, “Q”, and “M”, respectively; Mann-Whitney $P < 0.05$, adjusted $P > 0.1$ for all; **Supplementary Fig. 7c**). In the second half of pregnancy, the median dN/dS was significantly lower in sPTB pregnancies for lipid transport and metabolism and cell motility (COG categories “I” “N”; Mann-Whitney $P = 0.0040$ and $P = 0.04$, adjusted $P = 0.07$ and 0.40, respectively; **Fig. 3f**). No significant difference in the selection based on dN/dS was observed in non-*Gardnerella* phylogroups ($P > 0.05$ for all). Our results suggest that *Gardnerella* spp. genes involved in lipid transport and metabolism may undergo stronger purifying selection in sPTB. As purifying selection maintains the fitness of organisms by constantly sweeping away deleterious mutations and conserving functions, *Gardnerella* spp. may benefit from this stronger purifying selection targeting lipid functioning when growing in the sPTB-associated vaginal environment during pregnancy.

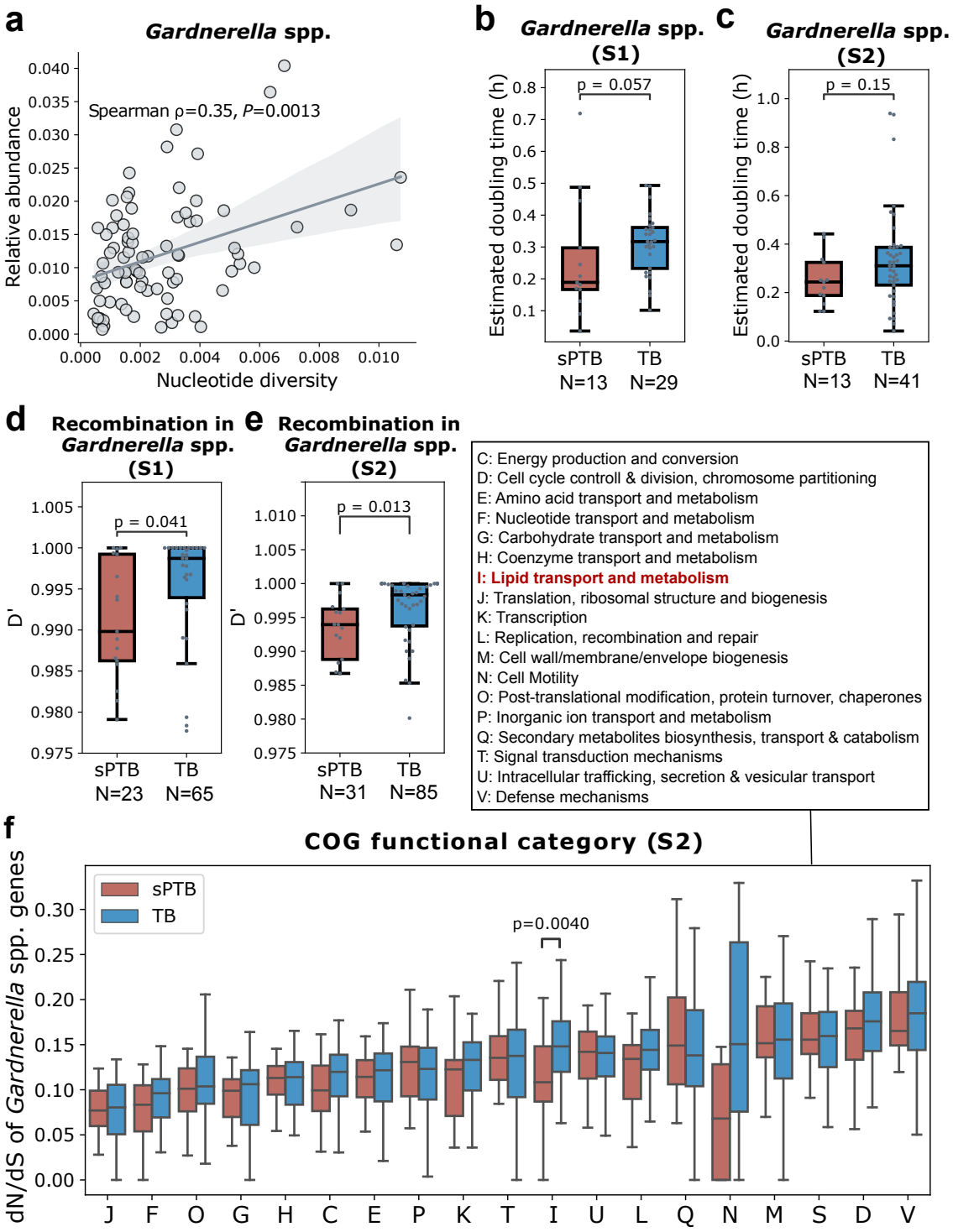

Fig. 3 | Evolutionary forces on *Gardnerella* spp. a. Spearman correlation between median genome-wide nucleotide diversity and relative abundance of *Gardnerella* spp. along pregnancy. The line and the shaded area depict the best-fit trendline and the 95% confidence interval (mean ± 1.96 s.e.m.) of the linear regression. **b,c,** Predicted maximal doubling time (gRodon[36]) of *Gardnerella* spp. compared between sPTB and TB, displayed for the first (b, S1) and second (c, S2) halves of pregnancy. Box, IQR; line, median; whiskers, 1.5*IQR; *p*, two-sided Mann-Whitney. **d,e,** Median D' of *Gardnerella* spp compared between sPTB and TB, displayed for the first (S1, **d**)

349 and second (S2, **e**) halves of pregnancy. Lower D' indicates more frequent recombination. **f,** dN/dS of
350 *Gardnerella* spp genes compared between sPTB and TB by COG functional categories, displayed for the second
351 half of pregnancy (S2). dN/dS closer to 0 indicates stronger purifying selection.
352
353 **sPTB-associated vaginal microbiomes have a higher antibiotic-resistance potential.**
354 Antibiotics are widely used during pregnancy, sometimes even topically in the vagina[48]. This exposure
355 may promote antimicrobial resistance (AMR). To assess if antibiotic-resistance potential in the vaginal
356 microbiome is associated with sPTB, we subsampled an identical number of reads (10^5) from each
357 sample and mapped them to the Comprehensive Antibiotic Resistance Database[49]. The total number of
358 reads mapped to AMR reference genes was significantly higher in the first half of sPTB pregnancies
359 (Mann-Whitney U $P = 0.015$; **Fig. 4a**), but not in the second half ($P = 0.76$; **Fig. 4b**). In addition, to
360 assess the difference of specific AMR genes between the vaginal microbiomes of sPTB and TB, we
361 identified AMR genes in the genomic assemblies. A significantly higher median count and Shannon-
362 Wiener diversity of AMR genes were detected in vaginal microbes sampled at the first half of
363 pregnancies that ended preterm (3-times higher on average; Mann-Whitney U $P = 0.011$ and $P =$
364 0.0078, respectively; ; **Fig. 4c and 4e**, respectively), yet this difference was not detected in the second
365 half ($P = 0.16$ for both; **Fig. 4d and 4f**, respectively). Exploring the source of these genes, we found a
366 significantly higher median fraction of phage-borne AMR genes in the microbiomes of women who
367 delivered preterm (one-sided $P = 0.016$, adjusted $P = 0.093$.; **Fig. 4g**), suggesting transduction may
368 promote the higher median count and diversity of AMR genes observed in the first half of sPTB
369 pregnancies (**Fig. 4c,e**). Among the 9 AMR gene categories that had genes present in at least 10% of
370 women, phenicol, aminoglycoside, glycopeptide, and MLS resistance genes showed a significantly
371 higher median fraction in the sPTB microbiome ($P < 0.05$, adjusted $P < 0.1$ for all; **Fig. 4h**). These
372 results suggest a unique antibiotic resistance profile associated with the first half of sPTB pregnancies,
373 potentially indicative of usage of specific antibiotics. Indeed, we detected a somewhat higher richness
374 of AMR genes along the first half of pregnancy in the 29 women who used antibiotics in the past 6
375 months before pregnancy than those who did not (Mann-Whitney U $P = 0.079$; **Fig. 4i**). This is also
376 consistent with our observation that genes with sPTB-associated nucleotide diversity were enriched for
377 drug metabolism in *G. swidsinskii* (PG044) (**Fig. 2d**).
378
379 As a higher risk of preterm birth has been reported to be associated with bacterial vaginosis (BV)[50–52],
380 and antibiotics used to treat BV may change the AMR genetic profiles of the vaginal microbiome, our
381 findings in AMR genes might be potentially confounded by BV. To assess this potential bias, we
382 compared AMR gene count between women with and without BV as well as between women with and
383 without BV history. We found that the AMR gene count was not significantly different between women
384 with and without BV for both halves of pregnancy ($P = 0.38$ and 0.5, respectively; **Supplementary Fig.**
385 **8a**). Similarly, it was not different between women with and without BV history ($P = 0.45$ and 0.1,
386 respectively; **Supplementary Fig. 8b**). These results suggest that the association between AMR gene
387 and pregnancy outcomes is independent of BV.
388
389 To check if the strong association between sPTB and the AMR potential of the vaginal microbiome is
390 contributed by a particular phylogroup, we performed a similar analysis for each phylogroup. We found,
391 however, that none of them showed a significant difference in the median count and diversity of AMR
392 genes between sPTB and TB (Mann-Whitney U $P > 0.05$ for all). This result suggests that the higher
393 AMR potential associated with sPTB may be a property of the vaginal microbiome as an ecosystem.

394 However, this lack of association could also be driven by underestimation of AMR genes due to the
395 limitation of MAG binning methods in recovering mobile genetic elements[53].

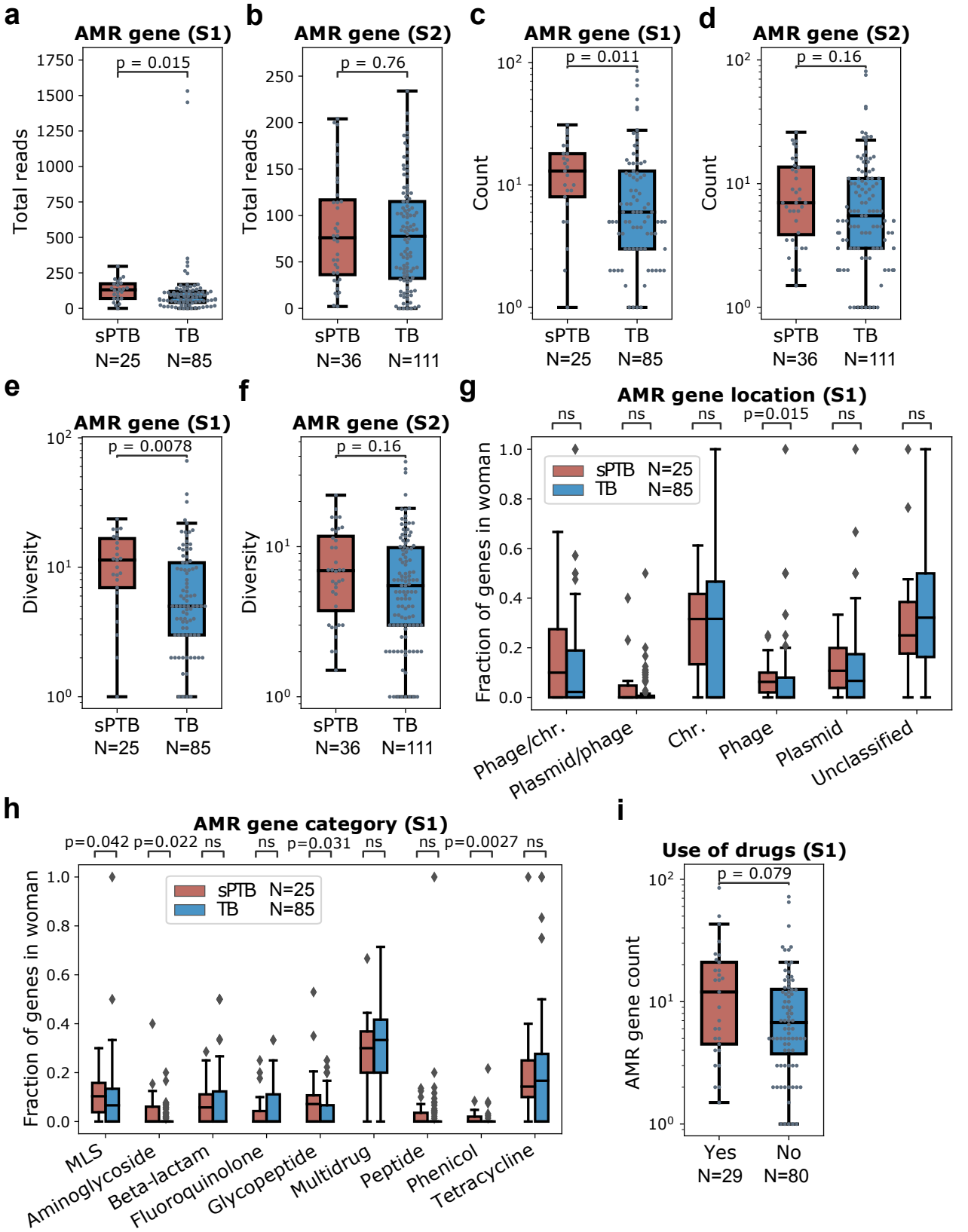

Fig. 4 | Antimicrobial resistance (AMR) gene profiles of the vaginal microbiome are associated with sPTB. a,b, Total subsampled reads (10^5) mapped to AMR genes compared between sPTB and TB, in the first (S1, **a**) and second (S2, **b**) halves of pregnancy. **c,d,** Median count (along period) of AMR genes compared between sPTB and TB, in the first (S1, **c**) and second (S2, **d**) halves of pregnancy**. e,f,** Median Shannon-Wiener diversity (along period) of AMR genes compared between sPTB and TB, in the first (S1, **e**) and second (S2, **f**) halves of pregnancy**. g,** Fraction of AMR genes originating in different locations, shown as median along the first half of each pregnancy. Chr.: chromosome. **h.** Fraction of AMR genes belonging to different resistance categories, shown as median along the first half of each pregnancy. MLS, macrolide, lincosamide and streptogramin B. **i.** AMR gene richness in the first half of pregnancy (S1) compared between women who used and did not use drugs in the past 6 months before pregnancy. Box, IQR; line, median; whiskers, 1.5*IQR; *p*, two-sided Mann-Whitney U.

Discussion

Microbial genomes can exhibit large variations even within the same species, as a result of adaptation to various environments[54]. Associations between the vaginal microbiome and preterm birth have been widely reported[7,8,12,35,52]. However, there is still much left to explore regarding potential mechanisms underlying host-microbiome interactions in this context. Here, by leveraging publicly available metagenomic data[1], we provide a population genetic view of the vaginal microbiome during pregnancy. We identify a number of novel microbial features including population nucleotide diversity, selection metrics, and antibiotic resistance potential that are associated with sPTB. Interestingly, we find that the higher population nucleotide diversity is driven by *Gardnerella* spp. during the first half of pregnancy. This species appears to undergo more intense changes in the population structure contributed by recombination and purifying selection in pregnancies which ended preterm. We also show evidence that this sPTB-associated genetic pattern of *Gardnerella* spp. may be related to optimization of growth rates in vaginal conditions linked to sPTB. Our results are indicative of adaptation of the vaginal microbiota to the host, which in turn may influence pregnancy outcomes.

Our findings regarding a relationship between ecological processes in the pregnancy vaginal microbiome and subsequent preterm birth are consistent with previous studies[1,7,11,12,14,52,55]. We add to these studies by exploring an additional layer of microbial variability associated with sPTB - microbial genetic diversity. It is known that genomic variation within species can result in phenotypic diversity and adaptations to different environments[54]. These adaptations, in turn, can affect host phenotypes such as disease outcomes[56]. Such associations between microbial genomic variation and host phenotypes have been reported in the gut microbiome[45,57,58]. Our study suggests that this phenomenon also occurs in the vaginal ecosystem, and that it may be associated with pregnancy outcomes. Nethertheless, the associations between microbial genetic diversity and pregnancy outcomes we detect might also be a consequence of different processes or unmeasured confounders that act on both variables (e.g., certain drugs or exogenous chemical compounds are that drive inflammation), and while we find this unlikely, this should be determined by future studies.

Interestingly, we found that the association of genetic diversity and sPTB was largely driven by *Gardnerella* spp., a group of species commonly associated with BV[50–52]. A number of studies reported a higher abundance of these species in sPTB pregnancies[1,9,52,59,60]. A recent preprint also demonstrated a higher number of *Gardnerella* clades in sPTB[61]. We show that *Gardnerella* spp. populations with more genetically diverse strains may also be associated with sPTB. In addition, we found that this taxon

442 has the capacity to grow 1.5 times faster in pregnancies that ended preterm, consistent with an overall
443 higher relative transcriptional rate of *G. vaginalis* which was previously reported[1]. These more
444 genetically diverse strains appear to have adapted to the vaginal environment associated with sPTB,
445 exhibiting higher fitness. Notably, the higher genetic diversity associated with sPTB in *Gardnerella* spp.
446 was detected during the first half of the pregnancy (<20 gestational week) rather than the second half.
447 The enriched nucleotide diversity during the first half of pregnancy might be related to the change of
448 human chorionic gonadotropin (HCG), which peaks at roughly the same time as *G. vaginalis*
449 microdiversity as we observed in **Fig. 2c**, and was suggested to play an immunomodulatory role in
450 humans[62,63]. To our knowledge, however, the effect of HCG on the vaginal ecosystem is not well
451 established yet. Most potential biomarkers of sPTB (e.g., serum alpha-fetoprotein[64] were so far
452 identified using samples from the second trimester of pregnancy (gestational week 14-27). Our results
453 suggest that high resolution analysis of microbiome samples from even earlier stages of pregnancy
454 (<week 20) may yield informative biomarkers of pregnancy outcomes.
455
456 As in the human gut microbiome[19–21], we show evidence that adaptive evolution also occurs in the
457 vaginal microbiome. Several environmental factors affecting the vaginal ecosystem, such as pH,
458 neutrophil levels, and xenobiotics, have been reported to be associated with sPTB[35,65]. These
459 environmental factors may act as selective stressors that lead to different evolutionary patterns in the
460 vaginal microbiome. Indeed, we detected more frequent homologous recombination and stronger
461 purifying selection within *Gardnerella* spp. during pregnancies that end preterm. Homologous
462 recombination is a critical mechanism speeding adaptation by increasing fixation probability of
463 beneficial mutations[66] and reducing clonal interference (i.e., competition between beneficial mutations)
464 in bacteria[67]. Purifying selection also contributes to adaptation by sweeping away deleterious mutations
465 and conserving functions, such as in oligotrophic nutrient conditions[44,68]. Notably, we found that sPTB-
466 associated purifying selection is particularly strong on genes involved in lipid transportation and
467 metabolism. This is consistent with previous identification of lipid metabolites (e.g., monoacylglycerols
468 and sphingolipids) as signatures of sPTB[35,69]. Whether this stronger purifying selection targeting lipid
469 transportation and metabolisms in pregnancy that ended preterm leads to changes in the
470 concentrations of lipid metabolites however requires further experimental testing. As both
471 recombination and purifying selection can reduce genetic diversity, sPTB-associated recombination and
472 purifying selection along pregnancy may explain the higher nucleotide diversity of *Gardnerella* spp. in
473 sPTB in the first half of pregnancy compared to the second half.
474
475 Antibiotics are common selective stresses acting on the human microbiome[29] and have been
476 associated with preterm birth[70]. We detected higher count and diversity of AMR genes associated with
477 sPTB, which our analysis suggests to be facilitated by prophages in preterm vaginal microbiomes.
478 While multiple phages (e.g., Siphoviridae, Myoviridae, and Microviridae) have been detected in the
479 vagina of pregnant women, their association with sPTB is rarely studied[71]. Our results imply a
480 potentially important role of bacteria-phage interactions in pregnancy outcomes via transferring of AMR
481 genes. We also found that genes related to phenicol and aminoglycoside resistance were more
482 abundant in vaginal microbiomes during pregnancies that ended preterm. While both antibiotics have
483 been frequently used to treat gynecologic infection for decades[72], and some phenicols (e.g.,
484 chloramphenicol) are thought to be safe for use during pregnancy[73] aminoglycoside is teratogenic.
485 Previous studies reported that exposure to antibiotics could change the composition of the vaginal
486 microbiome[48,74], indicating an ecological effect. In comparison, our results may suggest adaptation of
487 the vaginal microbiome to more frequent antibiotics usage in women who delivered preterm, leading to
488 an enrichment of AMR genes as well as higher nucleotide diversity in *Gardnerella* spp. genes encoding

enzymes for drug metabolism. While this hypothesis requires further study, it is further supported by the fact that a higher proportion of women who delivered preterm (31%) had used antibiotics in the past 6 months before pregnancy than women who delivered at term (23%).

Despite its findings, our study is limited by low sequencing depth (median bacterial read count < $5x10^5$) and inconsistent sampling frequency during pregnancy (1 to 8 samples per pregnancy, with an average of 4). These limitations lead to high sparsity in the features analyzed, preventing a more in-depth temporal and predictive analysis of the link between population genetics of the vaginal microbiome and sPTB. Our results warrant a high-resolution investigation of the vaginal metagenome, with frequent sampling and high sequencing depth.

In summary, through in-depth population genomic analyses, our study identified novel genetic and functional associations between the vaginal microbiome and preterm birth. We revealed evidence of microbial genetic adaptation to the host environment linked to preterm birth and highlighted the importance of microbial evolutionary processes to adverse pregnancy outcomes, particularly in *Gardnerella* spp.. Future investigation on the pressures driving the sPTB-associated microbial adaptation is warranted to fully understand the molecular mechanisms underlying preterm birth.

Methods

Sample selection and metagenomic data

This analysis was approved by the IRB of Columbia University (AAAS5367). We analyzed metagenomic sequencing data1 generated from the Multi-Omic Microbiome Study: Pregnancy Initiative (MOMS-PI) PTB case-control study which recruited a majority of women identifying as Black, which is described in ref. [1]. To this end, we obtained 135 vaginal samples collected longitudinally during pregnancy from 40 women who eventually delivered preterm spontaneously (sPTB) and 570 vaginal samples from 135 women who delivered at term (TB) from dbGaP (study no. 20280; accession phs001523.v1.p1). Samples were sequenced paired-end sequenced, to a mean±sd depth of 717,887±1,536,354 (mean ± s.d.) non-human reads. Fettweis et al. 2019[1] only included in this dataset term births after 39 weeks of gestation, with the intention of avoiding complications associated with early term birth[1]. Our study therefore uses the same definitions: spontaneous preterm birth is defined as live birth between 23 and 37 gestational weeks without medical indication, and term birth is defined as live birth at or after 39 gestational weeks.

On average, 3.36 and 3.21 samples were collected for each sPTB and TB woman, respectively (Mann-Whitney U P = 0.83); 1.68 and 1.51 samples were collected for the first half of pregnancy for each sPTB and TB woman, respectively (P = 0.30); and 2.34 and 2.14 samples were collected for the second half of pregnancy for each sPTB and TB woman, respectively (P = 0.27) (**Supplementary Table 2**). The average gestational age at the first sample being collected for sPTB and TB women is 17.38 and 16.09, respectively (P = 0.45), while for the last sample being collected for sPTB and TB women is 31.23 and 32.31, respectively (P = 0.72) (**Supplementary Table 2**). In addition, none of these women delivered at < 20 gestational weeks (**Supplementary Fig. 9a**). These indicate that dropping out due to late miscarriage/early PTB is not a concern to bias our findings in this study.

To check for the presence of some potential confounders for vaginal microbiome-sPTB associations, we calculated propensity scores[75] for each subject based on income, age, and race using a logistic regression model. We found that propensity scores for both sPTB and TB subjects exhibited a similar

535 distribution (Kolmogorov–Smirnov test $P = 0.21$), suggesting the associations we detect are not likely to
536 be confounded with these variables (**Supplementary Fig. 9b**). These results suggest a negligible
537 confounding effect of income, age, and race in this study on microbiome-sPTB associations. We note,
538 however, that population studies such as the one performed by Fettweis et al.[1] can be exposed to
539 selection bias, via access to medical care and other reasons. Experimental procedures for data
540 generation are described by Fettweis et al[1].
541
542 **Metagenomic assembly, genomic binning, genome annotation, and relative abundance**
543 Our analysis follows the accepted standards used in refs[76–79], using the ATLAS pipeline[80]. Bases with
544 quality scores <25, raw reads <50 bp lengths, and sequencing adapters were removed using
545 Trimmomatic v.0.39[81]. Reads mapped to human and PhiX genome sequences were removed by
546 mapping with Bowtie2 v.2.3.5.1[82]. Assembly and binning were done with ATLAS: filtered reads were
547 assembled using metaSPAdes v.3.15.2[83], and contigs were binned into metagenome-assembled
548 genomes (MAGs) using MetaBAT2 v.2.14.0 (ref. [84]) with a minimum contig length of 1500. Quality, GC
549 content, genome size, and taxonomy of MAGs were estimated using CheckM v.1.0.9[24]. MAGs were de-
550 replicated using dRep v.3.2.0[85] with an average nucleotide identity (ANI) of 0.95, minimum
551 completeness of 50%, and maximum genome contamination of 10%. The MAG with the highest dRep
552 score within each 95% ANI cluster, termed here as a phylogroup, was selected as the representative
553 MAGs for that phylogroup. Genes were predicted using Prodigal v.2.6.3[86] and annotated using
554 EggNOG v.5.0[87]. Filtered reads were mapped to representative MAGs using Bowtie2 v.2.3.5.1[88]. The
555 relative abundance of each representative MAG was calculated by dividing the number of reads that
556 mapped to that MAG, corrected to the genome size and completeness, by the total number of reads in
557 each sample.
558
559 **Phylogeny, ANI, and dendrogram**
560 Amino acid (AA) sequences of 120 marker genes were called and aligned for representative MAGs
561 using GTDB-Tk v.1.5.1 (ref. [89]). MAGs with <60% of AA in the alignment were excluded in the
562 phylogenetic tree construction. The best evolutionary model LG+G+I (the Le Gascuel model + gamma
563 distribution + invariant sites) was identified using prottest3 v.3.4.2 (ref. [90]) and 500 bootstraps were
564 used for tree construction using RAxML v.8.2.12 (ref. [91]). The tree was rooted by midpoint and
565 visualized in iTol v.6.3 (ref. [92]).
566 Pairwise ANI of MAGs for each phylogroup as well as for representative MAGs annotated as *G.*
567 *vaginalis* (PG42-53) and reference genomes of 13 *Gardnerella* species defined in ref. [25] was calculated
568 based on BLAST + using pyani. Dendrogram of ANI was constructed using the complete-linkage
569 clustering method in the vegan package in R v.3.6.0.
570
571 **Microdiversity profiling, growth rate estimation, and antimicrobial resistance genes**
572 Population microdiversity metrics including genome-wide nucleotide diversity, gene-wide nucleotide
573 diversity, linkage disequilibrium measures (D') and dN/dS, were calculated using InStrain v1.0.0[43] using
574 the 157 representative MAGs as the reference database. Maximal growth rate was estimated for each
575 MAG using gRodon[36]. Antimicrobial resistance (AMR) genes were detected in assemblies and MAGs
576 using PathoFact v.1.0 (ref. [93]) with default parameters.
577
578 **Temporal analysis**
579 To generate the trajectories representing the change in nucleotide diversity over time in term and preterm
580 deliveries, we pooled the temporal data of *Gardnerella* spp. from all women in each group (term and
581 preterm). When we had more than one observation per gestational week, we took the median value

across samples. We then binned the temporal data into bins of 3 weeks, except for the first bin which spanned weeks 1-7, and took the median of each bin as a summary. To smooth the observed binned data we applied splines, which is a special function defined piecewise by polynomials for data smoothing. To compare between the temporal trajectories of preterm and term, we performed a permutation test, in which we generated a null distribution of euclidean distances by shuffling the these trajectories 10^4 times and comparing to the euclidean distance in the original data[31].

Functional enrichment analysis

To identify COG/KEGG pathways that were enriched in genes showing significant difference in nucleotide diversity between sPTB and TB, the frequency of each COG/KEGG category was first calculated from significant genes (observed frequency). Then, the frequency of each COG/KEGG category was calculated from an identical number of genes randomly selected from all genes (expected frequency). This process was repeated 10,000 times. The null hypothesis was that the observed frequency of COG category is smaller than the expectation. For each COG, probability *P* of the null hypothesis was calculated using the formula: $P=|[x_i \in x : x_i >= k]| / 10000$, where [...] denotes a multiset, $x = (x_1, x_2, \ldots, x_n)$ is a list of expected values, and k is the observed value.

Statistical analysis

A different number of samples was available for each woman in the database. In our analyses, we therefore used the median along pregnancy (or its first or second half). The false-discovery rate procedure (FDR) of Benjamini and Hochberg (BH)[94] was used to correct for multiple testing. Adjusted $P < 0.1$ was used as the significance cutoff.

Data availability

The dataset used is available from dbGaP (phs001523), including raw fastq files and participant metadata. Access to additional fields can be requested through the RAMS Registry (https://ramsregistry.vcu.edu). Additional project information is available at the project's website (http://vmc.vcu.edu/momspi). The validation dataset was obtained from SRA, under accession PRJNA288562.

Code availability

Code to replicate all analyses is available from https://github.com/korem-lab/MOMs-PI_microdiversity_2023

Acknowledgements

We thank members of the Korem lab for useful discussions. This study was supported by the Eunice Kennedy Shriver National Institute of Child Health and Human Development (NICHD) of the National Institutes of Health under award number R01HD106017, the Program for Mathematical Genomics at Columbia University, and the CIFAR Azrieli Global Scholarship in the Humans & the Microbiome Program (T.K.). The dataset used was obtained from dbGaP (phs001523), using data provided by Gregory A. Buck, Ph.D. and colleagues and supported by NICHD (U54 HD080784) (G.A.B).

Author contributions

J.L. and T.K. designed the study. J.L., L.S., and J.A.U analyzed the data with input from T.K., M.S., and G.A.B. J.L. wrote the manuscript with input from L.S., T.K., M.S., B.Z. and G.A.B. G.A.B. assisted with data access and acquisition.

Competing interests

G.A.B. is a member of the Scientific Advisory Board of Juno, LTD., a startup biotech firm focused on using the vaginal microbiome to address issues of women's gynecologic and reproductive health. Juno had no involvement in the current study. Other authors declare no competing interests.

References

1. Fettweis, J. M. *et al.* The vaginal microbiome and preterm birth. *Nat. Med.* **25**, 1012–1021 (2019).
2. Tiensuu, H. *et al.* Risk of spontaneous preterm birth and fetal growth associates with fetal SLIT2. *PLoS Genet.* **15**, e1008107 (2019).
3. Walani, S. R. Global burden of preterm birth. *Int. J. Gynaecol. Obstet.* **150**, 31–33 (2020).
4. Goldenberg, R. L., Culhane, J. F., Iams, J. D. & Romero, R. Epidemiology and causes of preterm birth. *Lancet* **371**, 75–84 (2008).
5. Hong, X. *et al.* Genome-wide approach identifies a novel gene-maternal pre-pregnancy BMI interaction on preterm birth. *Nat. Commun.* **8**, 15608 (2017).
6. Hong, X. *et al.* Genome-wide association study identifies a novel maternal gene× stress interaction associated with spontaneous preterm birth. *Pediatr. Res.* 1–8 (2020).
7. DiGiulio, D. B. *et al.* Temporal and spatial variation of the human microbiota during pregnancy. *Proc. Natl. Acad. Sci. U. S. A.* **112**, 11060–11065 (2015).
8. Ravel, J. *et al.* Vaginal microbiome of reproductive-age women. *Proc. Natl. Acad. Sci. U. S. A.* **108 Suppl 1**, 4680–4687 (2011).
9. Tabatabaei, N. *et al.* Vaginal microbiome in early pregnancy and subsequent risk of spontaneous preterm birth: a case-control study. *BJOG* **126**, 349–358 (2019).
10. Chu, D. M., Seferovic, M., Pace, R. M. & Aagaard, K. M. The microbiome in preterm birth. *Best Pract. Res. Clin. Obstet. Gynaecol.* **52**, 103–113 (2018).
11. Freitas, A. C., Bocking, A., Hill, J. E., Money, D. M. & VOGUE Research Group. Increased richness and diversity of the vaginal microbiota and spontaneous preterm birth. *Microbiome* **6**, 117 (2018).
12. Stout, M. J. *et al.* Early pregnancy vaginal microbiome trends and preterm birth. *Am. J. Obstet. Gynecol.* **217**, 356.e1-356.e18 (2017).
13. Hyman, R. W. *et al.* Diversity of the vaginal microbiome correlates with preterm birth. *Reprod. Sci.* **21**, 32–40 (2014).
14. Feehily, C. *et al.* Shotgun sequencing of the vaginal microbiome reveals both a species and functional potential signature of preterm birth. *NPJ Biofilms Microbiomes* **6**, 50 (2020).
15. Kosti, I., Lyalina, S., Pollard, K. S., Butte, A. J. & Sirota, M. Meta-Analysis of Vaginal Microbiome Data Provides New Insights Into Preterm Birth. *Front. Microbiol.* **11**, 476 (2020).
16. Gupta, P., Singh, M. P. & Goyal, K. Diversity of Vaginal Microbiome in Pregnancy: Deciphering the Obscurity. *Front Public Health* **8**, 326 (2020).
17. Ceccarani, C. *et al.* Diversity of vaginal microbiome and metabolome during genital infections. *Sci. Rep.* **9**, 14095 (2019).

669 18. Chase, A. B., Weihe, C. & Martiny, J. B. H. Adaptive differentiation and rapid evolution of a soil
670 bacterium along a climate gradient. *Proc. Natl. Acad. Sci. U. S. A.* **118**, (2021).
671 19. Zhao, S. *et al.* Adaptive Evolution within Gut Microbiomes of Healthy People. *Cell Host Microbe* **25**,
672 656-667.e8 (2019).
673 20. Garud, N. R. & Pollard, K. S. Population Genetics in the Human Microbiome. *Trends Genet.* **36**,
674 53–67 (2020).
675 21. Garud, N. R., Good, B. H., Hallatschek, O. & Pollard, K. S. Evolutionary dynamics of bacteria in the
676 gut microbiome within and across hosts. *PLoS Biol.* **17**, e3000102 (2019).
677 22. Murovec, B., Deutsch, L. & Stres, B. Computational Framework for High-Quality Production and
678 Large-Scale Evolutionary Analysis of Metagenome Assembled Genomes. *Mol. Biol. Evol.* **37**, 593–
679 598 (2020).
680 23. Olm, M. R. *et al.* Consistent Metagenome-Derived Metrics Verify and Delineate Bacterial Species
681 Boundaries. *mSystems* **5**, (2020).
682 24. Parks, D. H., Imelfort, M., Skennerton, C. T., Hugenholtz, P. & Tyson, G. W. CheckM: assessing
683 the quality of microbial genomes recovered from isolates, single cells, and metagenomes. *Genome*
684 *Res.* **25**, 1043–1055 (2015).
685 25. Vaneechoutte, M. *et al.* Emended description of Gardnerella vaginalis and description of
686 Gardnerella leopoldii sp. nov., Gardnerella piotii sp. nov. and Gardnerella swidsinskii sp. nov., with
687 delineation of 13 genomic species within the genus Gardnerella. *Int. J. Syst. Evol. Microbiol.* **69**,
688 679–687 (2019).
689 26. Hill, J. E., Albert, A. Y. K. & the VOGUE Research Group. Resolution and Cooccurrence Patterns
690 of Gardnerella leopoldii, G. swidsinskii, G. piotii, and G. vaginalis within the Vaginal Microbiome.
691 *Infection and Immunity* **87**, (2019).
692 27. Martino, C. *et al.* Context-aware dimensionality reduction deconvolutes gut microbial community
693 dynamics. *Nat. Biotechnol.* **39**, 165–168 (2021).
694 28. Mendz, G. L., Petersen, R., Quinlivan, J. A. & Kaakoush, N. O. Potential involvement of
695 Campylobacter curvus and Haemophilus parainfluenzae in preterm birth. *BMJ Case Rep.* **2014**,
696 (2014).
697 29. Suzuki, T. A. & Ley, R. E. The role of the microbiota in human genetic adaptation. *Science* **370**,
698 (2020).
699 30. Ferris, M. J. *et al.* Association of Atopobium vaginae, a recently described metronidazole resistant
700 anaerobe, with bacterial vaginosis. *BMC Infect. Dis.* **4**, 5 (2004).
701 31. Danielsson, P.-E. Euclidean distance mapping. *Computer Graphics and Image Processing* **14**,
702 227–248 (1980).
703 32. Goltsman, D. S. A. *et al.* Metagenomic analysis with strain-level resolution reveals fine-scale
704 variation in the human pregnancy microbiome. *Genome Res.* **28**, 1467–1480 (2018).
705 33. Manrique, P., Dills, M. & Young, M. J. The Human Gut Phage Community and Its Implications for
706 Health and Disease. *Viruses* **9**, (2017).
707 34. Schwebke, J. R., Muzny, C. A. & Josey, W. E. Role of Gardnerella vaginalis in the pathogenesis of
708 bacterial vaginosis: a conceptual model. *J. Infect. Dis.* **210**, 338–343 (2014).
709 35. Kindschuh, W. F. *et al.* Preterm birth is associated with xenobiotics and predicted by the vaginal
710 metabolome. *Nat Microbiol* **8**, 246–259 (2023).
711 36. Weissman, J. L., Hou, S. & Fuhrman, J. A. Estimating maximal microbial growth rates from
712 cultures, metagenomes, and single cells via codon usage patterns. *Proc. Natl. Acad. Sci. U. S. A.*
713 **118**, (2021).
714 37. Korem, T. *et al.* Growth dynamics of gut microbiota in health and disease inferred from single
715 metagenomic samples. *Science* **4**, 1101–1106 (2015).
716 38. Joseph, T. A., Chlenski, P., Litman, A., Korem, T. & Pe'er, I. Accurate and robust inference of
717 microbial growth dynamics from metagenomic sequencing reveals personalized growth rates.

718 *Genome Res.* **32**, 558–568 (2022).
719 39. Achtman, M. & Wagner, M. Microbial diversity and the genetic nature of microbial species. *Nat.*
720 *Rev. Microbiol.* **6**, 431–440 (2008).
721 40. Bohr, L. L., Mortimer, T. D. & Pepperell, C. S. Lateral Gene Transfer Shapes Diversity of spp.
722 *Front. Cell. Infect. Microbiol.* **10**, 293 (2020).
723 41. Hudson, R. R. Linkage disequilibrium and recombination. *Handbook of statistical genetics* (2004).
724 42. Kryazhimskiy, S. & Plotkin, J. B. The population genetics of dN/dS. *PLoS Genet.* **4**, e1000304
725 (2008).
726 43. Olm, M. R. *et al.* inStrain profiles population microdiversity from metagenomic data and sensitively
727 detects shared microbial strains. *Nat. Biotechnol.* **39**, 727–736 (2021).
728 44. Shenhav, L. & Zeevi, D. Resource conservation manifests in the genetic code. *Science* **370**, 683–
729 687 (2020).
730 45. Schloissnig, S. *et al.* Genomic variation landscape of the human gut microbiome. *Nature* **493**, 45–
731 50 (2013).
732 46. He, M. *et al.* Evolutionary dynamics of Clostridium difficile over short and long time scales. *Proc.*
733 *Natl. Acad. Sci. U. S. A.* **107**, 7527–7532 (2010).
734 47. Tatusov, R. L., Galperin, M. Y., Natale, D. A. & Koonin, E. V. The COG database: a tool for
735 genome-scale analysis of protein functions and evolution. *Nucleic Acids Res.* **28**, 33–36 (2000).
736 48. Stokholm, J. *et al.* Antibiotic use during pregnancy alters the commensal vaginal microbiota. *Clin.*
737 *Microbiol. Infect.* **20**, 629–635 (2014).
738 49. Alcock, B. P. *et al.* CARD 2020: antibiotic resistome surveillance with the comprehensive antibiotic
739 resistance database. *Nucleic Acids Res.* **48**, D517–D525 (2020).
740 50. Pace, R. M. *et al.* Complex species and strain ecology of the vaginal microbiome from pregnancy
741 to postpartum and association with preterm birth. *Med* **2**, 1027–1049 (2021).
742 51. Brown, R. G. *et al.* Vaginal dysbiosis increases risk of preterm fetal membrane rupture, neonatal
743 sepsis and is exacerbated by erythromycin. *BMC Med.* **16**, 9 (2018).
744 52. Callahan, B. J. *et al.* Replication and refinement of a vaginal microbial signature of preterm birth in
745 two racially distinct cohorts of US women. *Proc. Natl. Acad. Sci. U. S. A.* **114**, 9966–9971 (2017).
746 53. Maguire, F. *et al.* Metagenome-assembled genome binning methods with short reads
747 disproportionately fail for plasmids and genomic Islands. *Microb Genom* **6**, (2020).
748 54. Liao, J. *et al.* Nationwide genomic atlas of soil-dwelling Listeria reveals effects of selection and
749 population ecology on pangenome evolution. *Nat Microbiol* **6**, 1021–1030 (2021).
750 55. Haque, M. M., Merchant, M., Kumar, P. N., Dutta, A. & Mande, S. S. First-trimester vaginal
751 microbiome diversity: A potential indicator of preterm delivery risk. *Sci. Rep.* **7**, 16145 (2017).
752 56. Leung, J. M., Graham, A. L. & Knowles, S. C. L. Parasite-Microbiota Interactions With the
753 Vertebrate Gut: Synthesis Through an Ecological Lens. *Frontiers in Microbiology* vol. 9 Preprint at
754 https://doi.org/10.3389/fmicb.2018.00843 (2018).
755 57. Morowitz, M. J. *et al.* Strain-resolved community genomic analysis of gut microbial colonization in a
756 premature infant. *Proceedings of the National Academy of Sciences* vol. 108 1128–1133 Preprint
757 at https://doi.org/10.1073/pnas.1010992108 (2011).
758 58. Zeevi, D. *et al.* Structural variation in the gut microbiome associates with host health. *Nature* vol.
759 568 43–48 Preprint at https://doi.org/10.1038/s41586-019-1065-y (2019).
760 59. Menard, J. P. *et al.* High vaginal concentrations of Atopobium vaginae and Gardnerella vaginalis in
761 women undergoing preterm labor. *Obstet. Gynecol.* **115**, 134–140 (2010).
762 60. Kumar, S. *et al.* The Vaginal Microbial Signatures of Preterm Birth Delivery in Indian Women.
763 *Front. Cell. Infect. Microbiol.* **11**, 622474 (2021).
764 61. Berman, H. L., Aliaga Goltsman, D. S., Anderson, M., Relman, D. A. & Callahan, B. J. *Gardnerella*
765 diversity and ecology in pregnancy and preterm birth. *bioRxiv* 2023.02.03.527032 (2023)

766 doi:10.1101/2023.02.03.527032.
767 62. Schumacher, A. *et al.* Human chorionic gonadotropin attracts regulatory T cells into the fetal-
768 maternal interface during early human pregnancy. *J. Immunol.* **182**, 5488–5497 (2009).
769 63. Polese, B. *et al.* The Endocrine Milieu and CD4 T-Lymphocyte Polarization during Pregnancy.
770 *Front. Endocrinol.* **5**, (2014).
771 64. Yuan, W., Chen, L. & Bernal, A. L. Is elevated maternal serum alpha-fetoprotein in the second
772 trimester of pregnancy associated with increased preterm birth risk? *European Journal of*
773 *Obstetrics & Gynecology and Reproductive Biology* **145**, 57–64 (2009).
774 65. Simhan, H. N., Caritis, S. N., Krohn, M. A. & Hillier, S. L. Elevated vaginal pH and neutrophils are
775 associated strongly with early spontaneous preterm birth. *Am. J. Obstet. Gynecol.* **189**, 1150–1154
776 (2003).
777 66. Otto, S. P. & Barton, N. H. The evolution of recombination: removing the limits to natural selection.
778 *Genetics* **147**, 879–906 (1997).
779 67. Cooper, T. F. Recombination speeds adaptation by reducing competition between beneficial
780 mutations in populations of Escherichia coli. *PLoS Biol.* **5**, e225 (2007).
781 68. Martinez-Gutierrez, C. A. & Aylward, F. O. Strong Purifying Selection Is Associated with Genome
782 Streamlining in Epipelagic Marinimicrobia. *Genome Biol. Evol.* **11**, 2887–2894 (2019).
783 69. Gerson, K. D. *et al.* A non-optimal cervicovaginal microbiota in pregnancy is associated with a
784 distinct metabolomic signature among non-Hispanic Black individuals. *Sci. Rep.* **11**, 22794 (2021).
785 70. Terzic, M. *et al.* Periodontal Pathogens and Preterm Birth: Current Knowledge and Further
786 Interventions. *Pathogens* **10**, (2021).
787 71. da Costa, A. C. *et al.* Identification of bacteriophages in the vagina of pregnant women: a
788 descriptive study. *BJOG* **128**, 976–982 (2021).
789 72. Bargaza, R. A. & Cunha, B. A. Aminoglycosides in gynecology. *Int. Urogynecol. J.* **3**, 197–207
790 (1992).
791 73. Amstey, M. S. Chloramphenicol therapy in pregnancy. *Clinical infectious diseases: an official*
792 *publication of the Infectious Diseases Society of America* vol. 30 237 (2000).
793 74. Rick, A.-M. *et al.* Group B Streptococci Colonization in Pregnant Guatemalan Women: Prevalence,
794 Risk Factors, and Vaginal Microbiome. *Open Forum Infect Dis* **4**, ofx020 (2017).
795 75. Rosenbaum, P. R. & Rubin, D. B. The central role of the propensity score in observational studies
796 for causal effects. *Biometrika* **70**, 41–55 (1983).
797 76. Gálvez, E. J. C. *et al.* Distinct Polysaccharide Utilization Determines Interspecies Competition
798 between Intestinal Prevotella spp. *Cell Host Microbe* **28**, 838-852.e6 (2020).
799 77. Yang, S., Liebner, S., Svenning, M. M. & Tveit, A. T. Decoupling of microbial community dynamics
800 and functions in Arctic peat soil exposed to short term warming. *Mol. Ecol.* **30**, 5094–5104 (2021).
801 78. Kieser, S., Zdobnov, E. M. & Trajkovski, M. Comprehensive mouse microbiota genome catalog
802 reveals major difference to its human counterpart. *PLoS Comput. Biol.* **18**, e1009947 (2022).
803 79. Chevalier, C. *et al.* Warmth Prevents Bone Loss Through the Gut Microbiota. *Cell Metab.* **32**, 575-
804 590.e7 (2020).
805 80. Kieser, S., Brown, J., Zdobnov, E. M., Trajkovski, M. & McCue, L. A. ATLAS: a Snakemake
806 workflow for assembly, annotation, and genomic binning of metagenome sequence data. *BMC*
807 *Bioinformatics* **21**, 257 (2020).
808 81. Bolger, A. M., Lohse, M. & Usadel, B. Trimmomatic: a flexible trimmer for Illumina sequence data.
809 *Bioinformatics* **30**, 2114–2120 (2014).
810 82. Langmead, B. & Salzberg, S. L. Fast gapped-read alignment with Bowtie 2. *Nat. Methods* **9**, 357–
811 359 (2012).
812 83. Nurk, S., Meleshko, D., Korobeynikov, A. & Pevzner, P. A. metaSPAdes: a new versatile
813 metagenomic assembler. *Genome Res.* **27**, 824–834 (2017).

814 84. Kang, D. D. *et al.* MetaBAT 2: an adaptive binning algorithm for robust and efficient genome
815 reconstruction from metagenome assemblies. *PeerJ* **7**, e7359 (2019).
816 85. Olm, M. R., Brown, C. T., Brooks, B. & Banfield, J. F. dRep: a tool for fast and accurate genomic
817 comparisons that enables improved genome recovery from metagenomes through de-replication.
818 *ISME J.* **11**, 2864–2868 (2017).
819 86. Hyatt, D. *et al.* Prodigal: prokaryotic gene recognition and translation initiation site identification.
820 *BMC Bioinformatics* **11**, 119 (2010).
821 87. Huerta-Cepas, J. *et al.* eggNOG 5.0: a hierarchical, functionally and phylogenetically annotated
822 orthology resource based on 5090 organisms and 2502 viruses. *Nucleic Acids Res.* **47**, D309–
823 D314 (2019).
824 88. Danecek, P. *et al.* Twelve years of SAMtools and BCFtools. *Gigascience* **10**, (2021).
825 89. Chaumeil, P.-A., Mussig, A. J., Hugenholtz, P. & Parks, D. H. GTDB-Tk: a toolkit to classify
826 genomes with the Genome Taxonomy Database. *Bioinformatics* **36**, 1925–1927 (2019).
827 90. Darriba, D., Taboada, G. L., Doallo, R. & Posada, D. ProtTest 3: fast selection of best-fit models of
828 protein evolution. *Bioinformatics* **27**, 1164–1165 (2011).
829 91. Stamatakis, A. RAxML version 8: a tool for phylogenetic analysis and post-analysis of large
830 phylogenies. *Bioinformatics* **30**, 1312–1313 (2014).
831 92. Letunic, I. & Bork, P. Interactive Tree Of Life (iTOL) v5: an online tool for phylogenetic tree display
832 and annotation. *Nucleic Acids Res.* **49**, W293–W296 (2021).
833 93. de Nies, L. *et al.* PathoFact: a pipeline for the prediction of virulence factors and antimicrobial
834 resistance genes in metagenomic data. *Microbiome* **9**, 49 (2021).
835 94. Benjamini, Y. & Hochberg, Y. Controlling the false discovery rate: A practical and powerful
836 approach to multiple testing. *J. R. Stat. Soc.* **57**, 289–300 (1995).

837 **Supplementary figures**

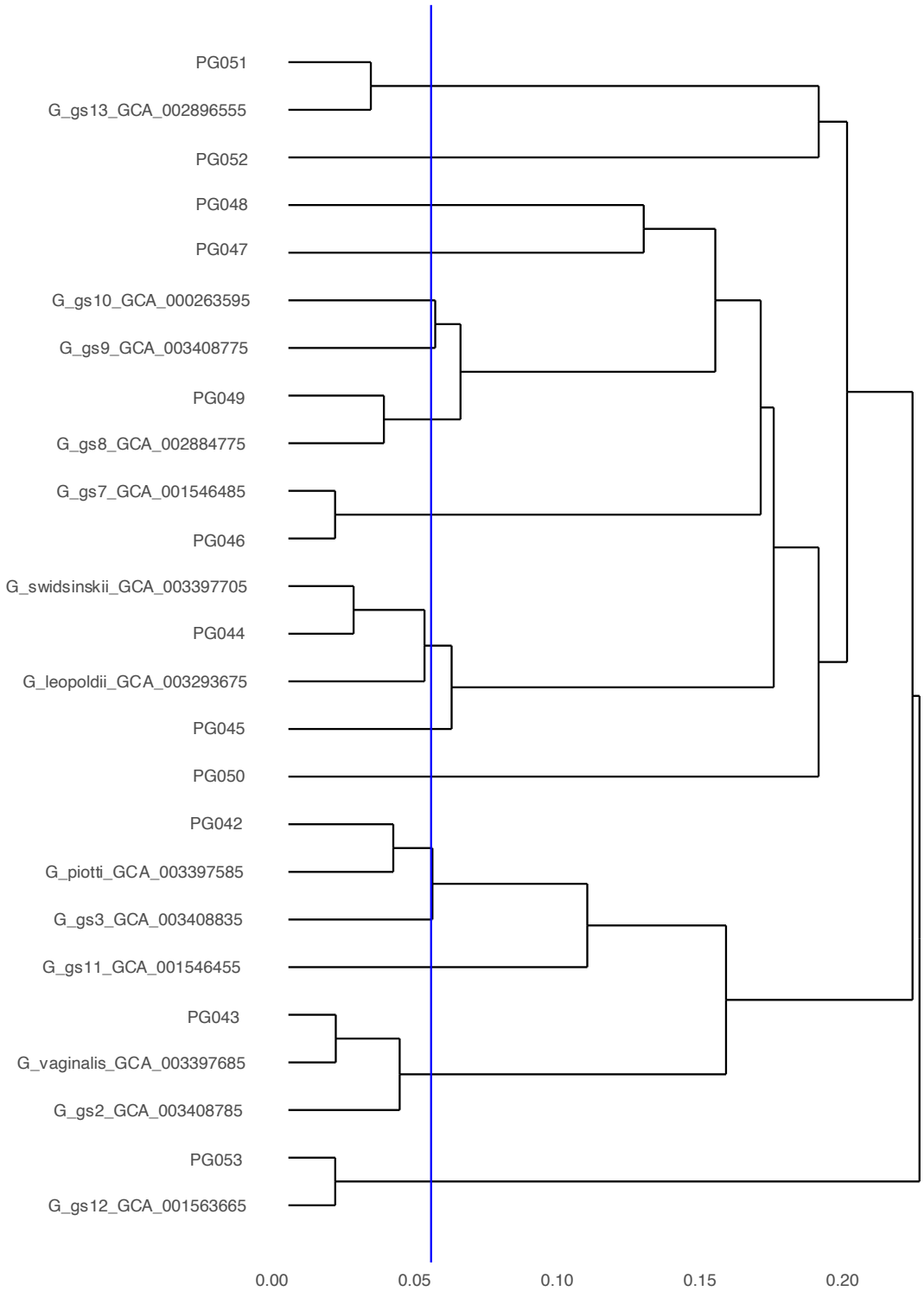

838

839 **Supplementary Fig. 1 | Dendrogram of representative MAGs annotated as *G. vaginalis* (PG42-53)**
840 **and reference genomes of 13 *Gardnerella* species defined in ref. [25] based on ANI.** Blue line shows
841 an ANI value of 0.95, which is a cutoff for prokaryotes species.

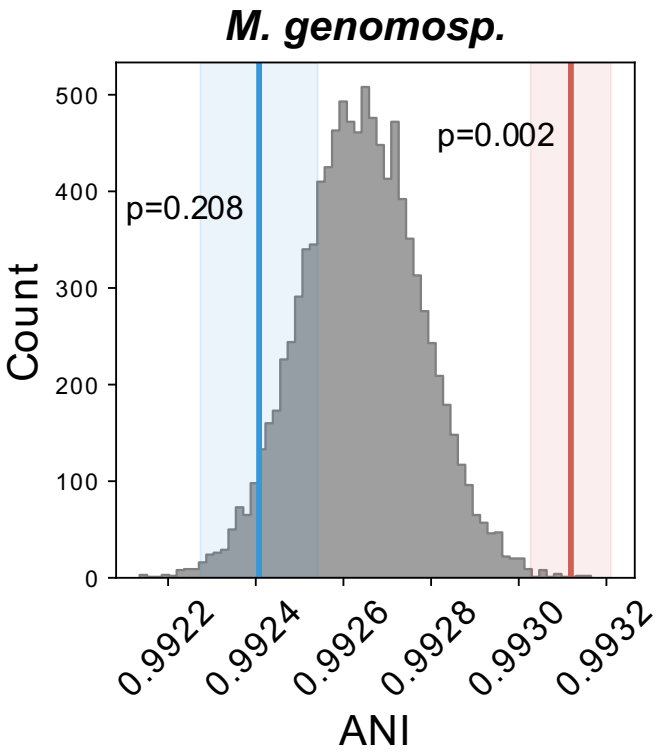

842
843 **Supplementary Fig. 2 | The distribution of average inter-host nucleotide identity (ANI) of MAGs classified as**
844 ***M. genomosp*.** The gray histogram illustrates the null distribution. The red and blue line and shaded area
845 indicate the average value and standard deviation of ANI observed in sPTB and in TB, respectively, calculated
846 from 10,000 repetitions; *p*, significance.

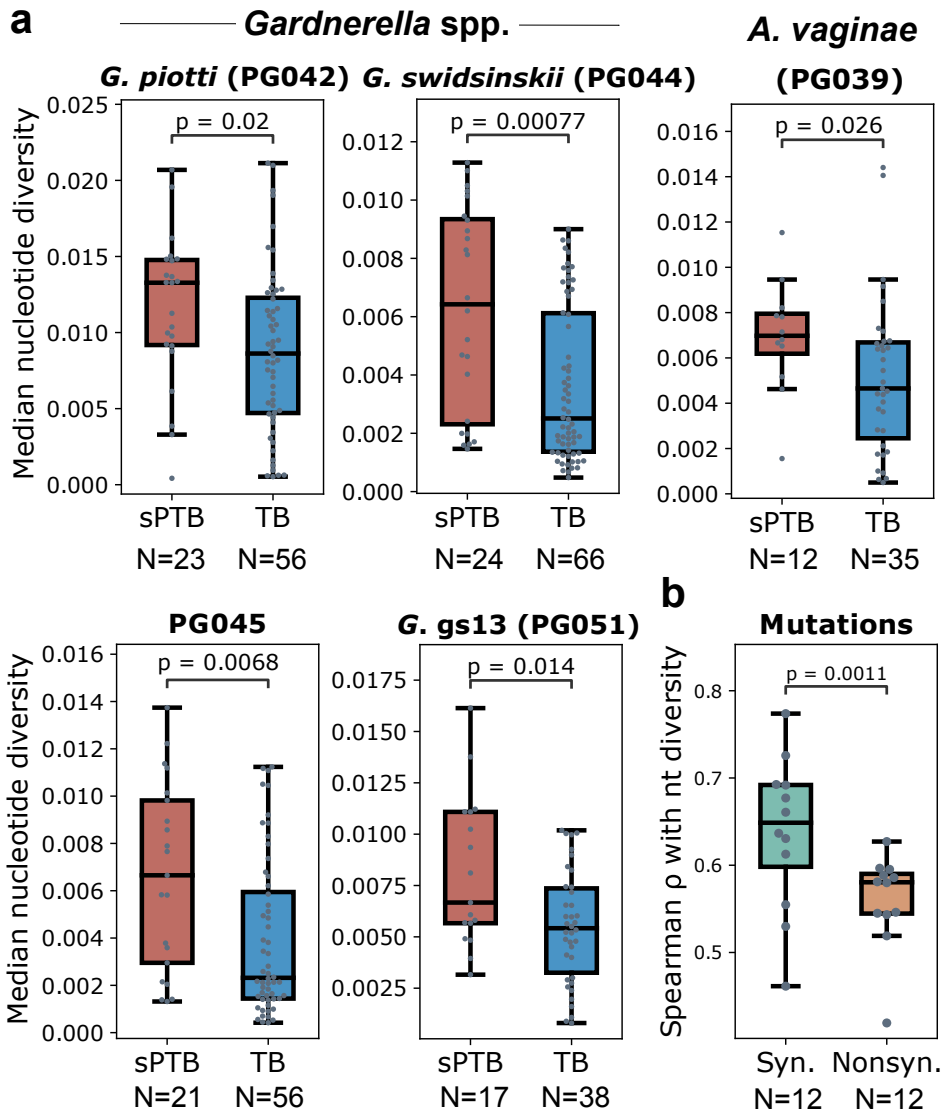

Supplementary Fig. 3 | Nucleotide diversity of vaginal microbial populations. a. Median genome-wide nucleotide diversity along pregnancies of four *Gardnerella* spp. phylogroups and a phylogroup classified as *A. vaginae*, compared between sPTB and TB. *p*, two-sided Mann-Whitney U. **b.** Spearman correlation coefficient between nucleotide diversity and number of synonymous mutations and nonsynonymous mutations of genes across 12 *Gardnerella* spp. phylogroups. Median spearman correlation coefficient of genes of each phylogroup based on median gene nucleotide diversity along pregnancy, compared between synonymous (Syn.) mutations and nonsynonymous (Nonsyn.) mutations. *p*, two-sided Student T test. Box, IQR; line, median; whiskers, 1.5*IQR.

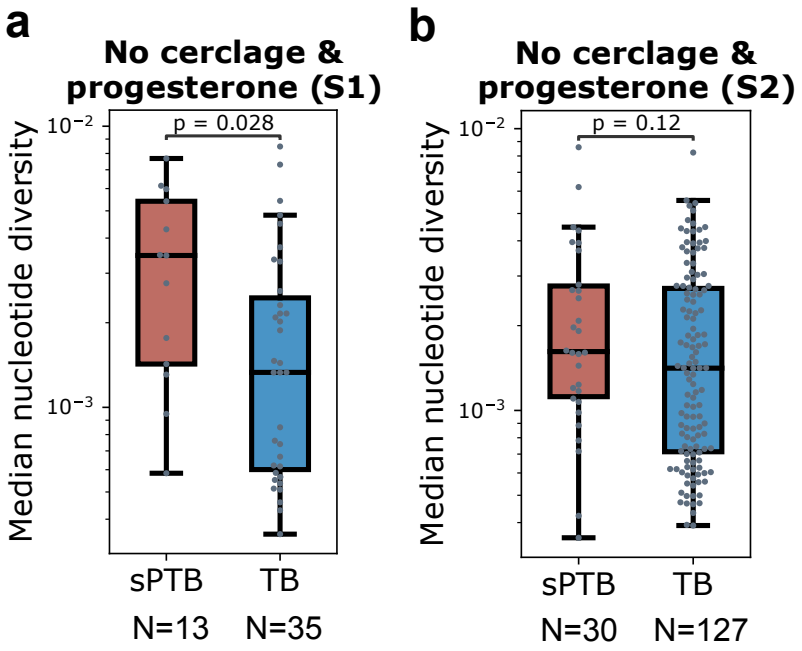

Supplementary Fig. 4 | The association between microdiversity and sPTB is not biased by medical interventions for risk of preterm birth, including cerclage and progesterone. a, b, A comparison of median genome-wide nucleotide diversity of *Gardnerella* spp. between sPTB and TB, , for women who did not receive cerclage nor progesterone during pregnancy, displayed for pregnancy S1 (a) and S2 (b). Box, IQR; line, median; whiskers, 1.5*IQR; *p*, two-sided Mann-Whitney.

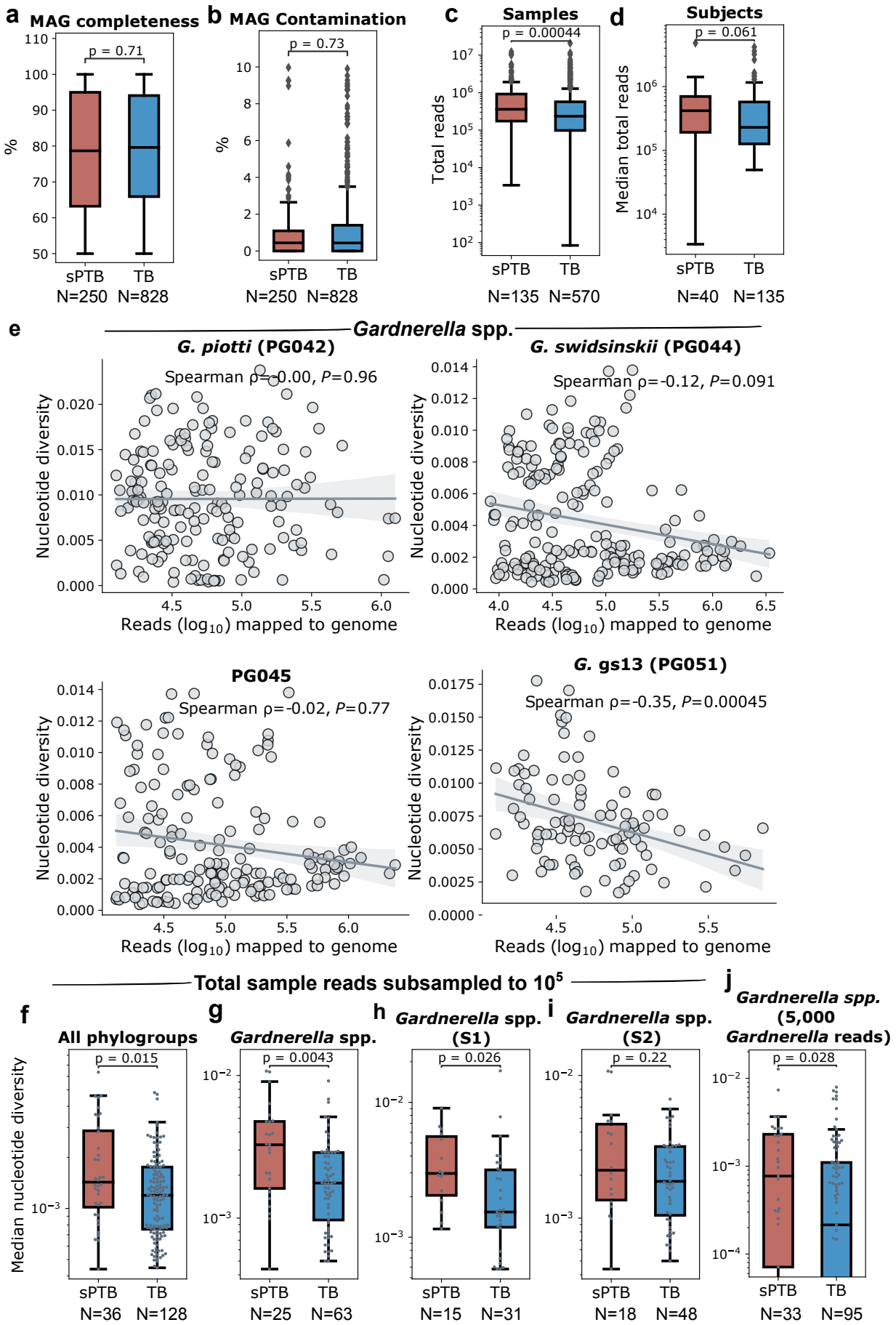
a
MAG completeness
p = 0.71
%
sPTB
TB
N=250
N=828
b
MAG Contamination
p = 0.73
%
sPTB
TB
N=250
N=828
c
Samples
p = 0.00044
Total reads
sPTB
TB
N=135
N=570
d
Subjects
p = 0.061
Median total reads
sPTB
TB
N=40
N=135
e
Gardnerella spp.
G. piotti (PG042)
Spearman ρ=-0.00, P=0.96
Nucleotide diversity
Reads (log10) mapped to genome
G. swidsinskii (PG044)
Spearman ρ=-0.12, P=0.091
Nucleotide diversity
Reads (log10) mapped to genome
PG045
Spearman ρ=-0.02, P=0.77
Nucleotide diversity
Reads (log10) mapped to genome
G. gs13 (PG051)
Spearman ρ=-0.35, P=0.00045
Nucleotide diversity
Reads (log10) mapped to genome
Total sample reads subsampled to 10^5
f
All phylogroups
p = 0.015
Median nucleotide diversity
sPTB
TB
N=36
N=128
g
Gardnerella spp.
p = 0.0043
sPTB
TB
N=25
N=63
h
Gardnerella spp. (S1)
p = 0.026
sPTB
TB
N=15
N=31
i
Gardnerella spp. (S2)
p = 0.22
sPTB
TB
N=18
N=48
j
Gardnerella spp. (5,000 Gardnerella reads)
p = 0.028
sPTB
TB
N=33
N=95

862 **Supplementary Fig. 5 | The association between microdiversity and sPTB is not biased by sequencing depth.**
863 **a,b,** Completeness (a) and contamination (b) of MAGs, compared between sPTB and TB. **c,d,** Total read counts of
864 samples (c) and median read count (d) along each pregnancy compared between sPTB and TB. **e,** Spearman
865 correlation between genome-wide nucleotide diversity and reads mapped to each of the four *Gardnerella* spp.
866 phylogroups that show difference in nucleotide diversity between sPTB and TB in **Fig. S2a**. The line and the
867 shaded area depict the best-fit trendline and the 95% confidence interval (mean ± 1.96 s.e.m.) of the linear
868 regression. **f,g,** Median genome-wide nucleotide diversity along pregnancy of all phylogroups (f) and *Gardnerella*
869 spp. (g), compared between sPTB and TB based on 10^5 reads sampled from each sample. **h,i,** Median genome-
870 wide nucleotide diversity of *Gardnerella* spp. along the first (S1, h) and second (S2, i) halves of pregnancy,
871 compared between sPTB and TB based on 10^5 reads sampled from each sample. Box, IQR; line, median;
872 whiskers, 1.5*IQR; *p*, two-sided Mann-Whitney. **j.** Median genome-wide nucleotide diversity along pregnancy of
873 *Gardnerella* spp., compared between sPTB and TB based on 5,000 reads mapped to *Gardnerella* spp. sampled
874 from each sample.
875
876
877

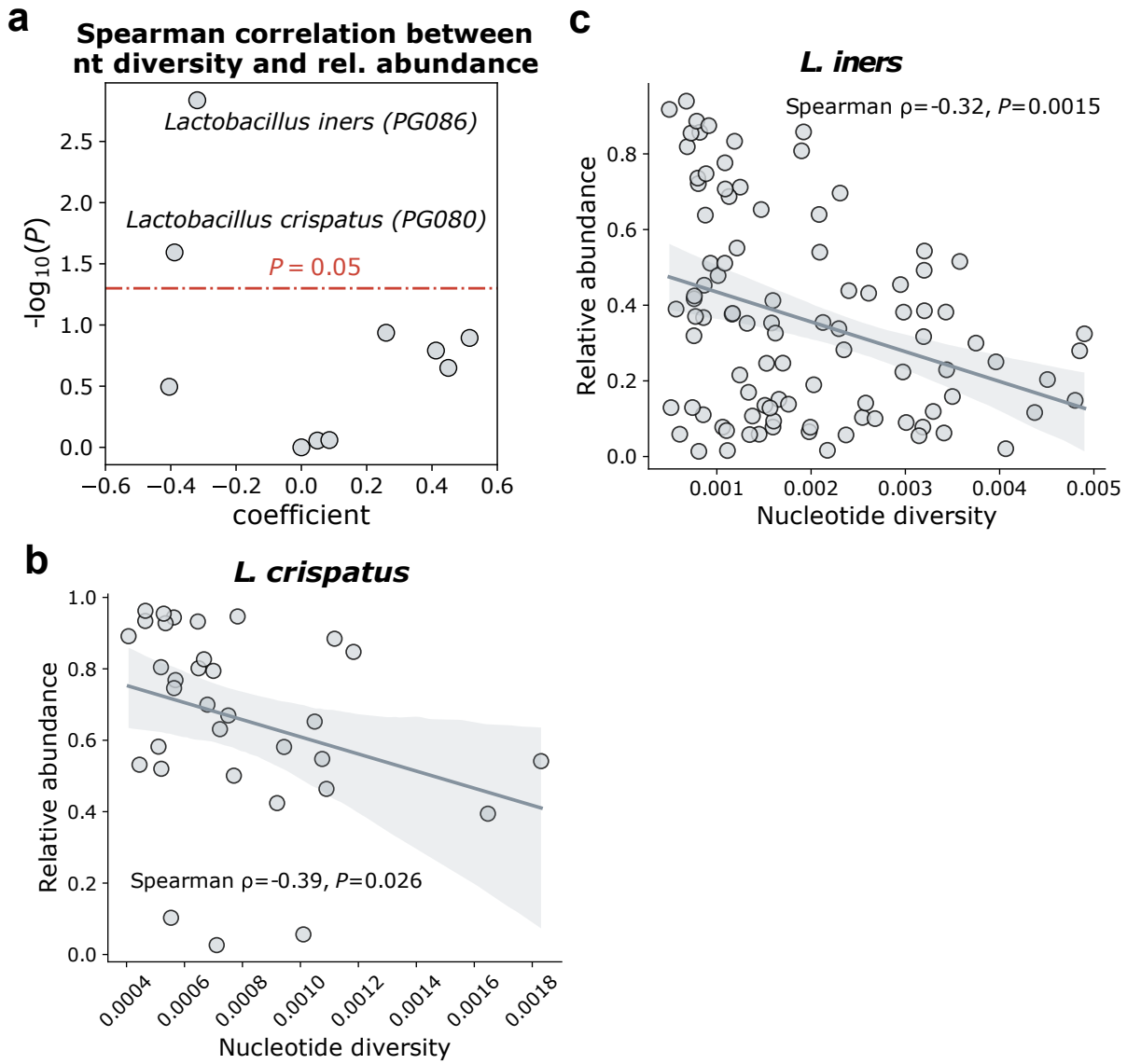

Supplementary Fig. 6 | Spearman correlation between genome-wide nucleotide diversity and relative abundance of non-*Gardnerella* phylogroups. a. Volcano plot illustrating the Spearman correlation (significance, y-axis; coefficient, x-axis) between median genome-wide nucleotide diversity and relative abundance along pregnancies. Phylogroups above the red dashed line have a $P < 0.05$. **b,c,** Spearman correlation between median genome-wide nucleotide diversity and relative abundance of *L. crispatus* (b) and *L. iners* (c) along pregnancy. The line and the shaded area depict the best-fit trendline and the 95% confidence interval (mean ± 1.96 s.e.m.) of the linear regression.

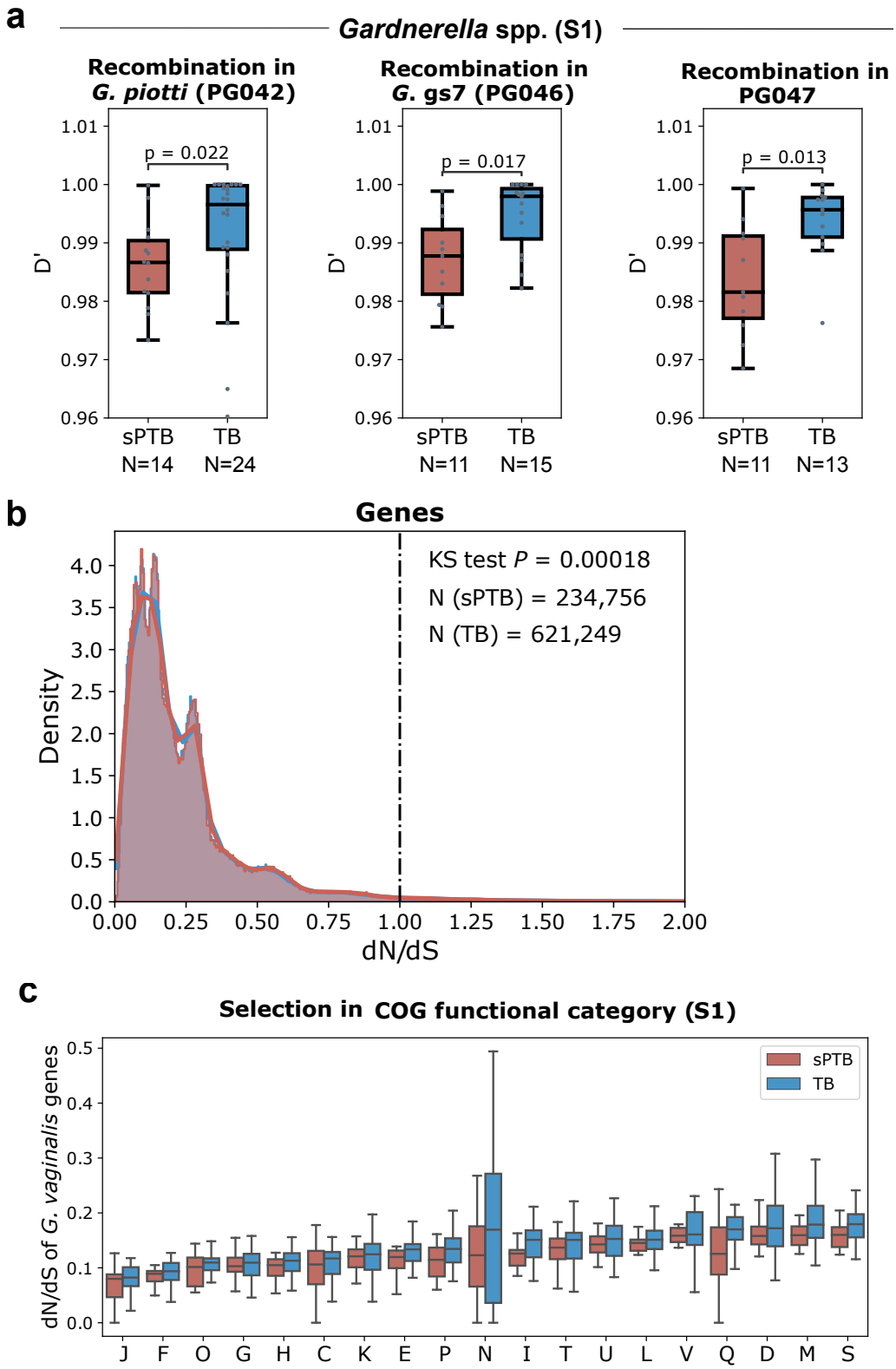

Supplementary Fig. 7 | Evolutionary forces on the vaginal microbiome. a. Median D' along the first half of pregnancy (S1) of *Gardnerella* spp. phylogroups compared between sPTB and TB. Lower D' indicates more frequent recombination. Box, IQR; line, median; whiskers, 1.5*IQR; *P*, two-sided Mann-Whitney. **b.** Density of median (along pregnancy) of dN/dS of genes in sPTB (red) and in TB (blue). *P*: Kolmogorov–Smirnov (KS) test. **c.** dN/dS of *Gardnerella* spp. genes compared between sPTB and TB by COG functional categories, displayed for

891 the first (S1, **c**) half of pregnancy. C, Energy production and conversion; D, Cell cycle control, cell division,
892 chromosome partitioning; E, Amino acid transport and metabolism; F, Nucleotide transport and metabolism; G,
893 Carbohydrate transport and metabolism; H, Coenzyme transport and metabolism; I, Lipid transport and
894 metabolism; J, Translation, ribosomal structure and biogenesis; K, Transcription; L, Replication, recombination
895 and repair; M, Cell wall/membrane/envelope biogenesis; N, Cell Motility, O: Post-translational modification,
896 protein turnover, chaperones; P, Inorganic ion transport and metabolism; Q, Secondary metabolites
897 biosynthesis, transport and catabolism; T, Signal transduction mechanisms; U, Intracellular trafficking, secretion,
898 and vesicular transport; V, Defense mechanisms.
899

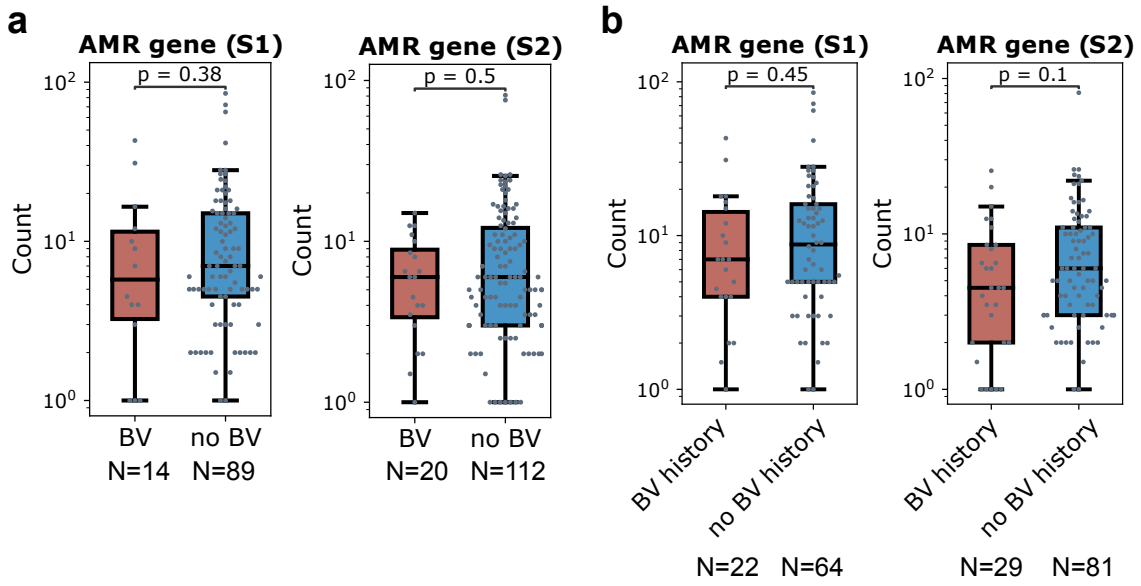

Supplementary Fig. 8 | Antimicrobial resistance (AMR) gene profiles of the vaginal microbiome are not associated with bacterial vaginosis (BV). a,b, Median count (along period) of AMR genes in the first (S1) and second (S2) halves of pregnancy, compared between women with and without BV (**a**) and between women with and without BV history (**b**)**.** Box, IQR; line, median; whiskers, 1.5*IQR; *p*, two-sided Mann-Whitney U.

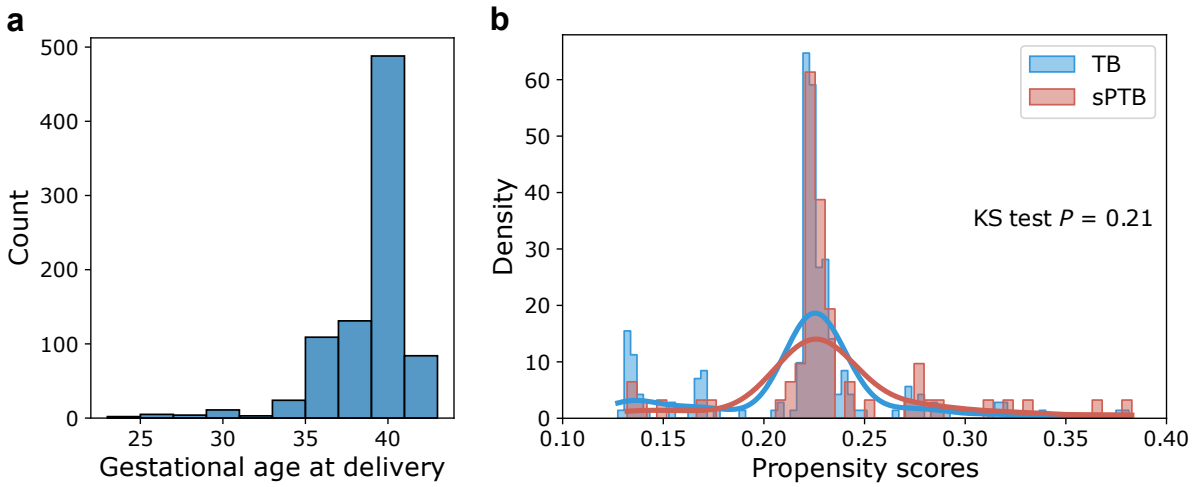

905 **Supplementary Fig. 9 | Sample summary. a.** Histogram showing the distribution of gestational age of women
906 at delivery. **b.** Distribution of propensity scores of women groups based on income, age, and race using a logistic
907 regression model. The histogram is smoothed using a kernel. sPTB: red, TB: blue, *P*: Kolmogorov–Smirnov (KS)
908 test.
909

Supplementary tables

Supplementary Table 1 Genome assembly features of representative MAGs for phylogroups and taxonomy.

Supplementary Table 2 Summary of longitudinal samples collected during pregnancy for women who deliver spontaneous preterm (sPTB) and at term (TB).

	sPTB	TB	Mann-Whitney U *P*
N of samples / woman (mean ± s.d.)	3.36 ± 1.51	3.21 ± 1.13	0.83
N of samples / woman for the first half of pregnancy (mean ± s.d.)	1.68 ± 0.69	1.51 ± 0.56	0.30
N of samples / woman for the second half of pregnancy (mean ± s.d.)	2.34 ± 1.10	2.14 ± 0.90	0.27
Gestational age at the first sample (mean ± s.d.)	17.38 ± 8.08	16.09 ± 7.50	0.45
Gestational age at the last sample (mean ± s.d.)	31.23 ± 5.52	32.31 ± 3.66	0.72

Supplementary Table 3 eggNOG functional annotation of genes.

Supplementary Table 4 STORMS checklist.